Paper:
Rezaei, M., Fazelzadeh, S., Mazidi, A. & Khodaparast, H. (2018). Fuzzy uncertainty analysis in the flutter boundary of an aircraft wing subjected to a thrust force. *Proceedings of the Institution of Mechanical Engineers, Part G: Journal of Aerospace Engineering*, 095441001877389
http://dx.doi.org/10.1177/0954410018773898

Fuzzy uncertainty analysis in the flutter boundary of an aircraft wing subjected to a thrust force

Journal:	*Part G: Journal of Aerospace Engineering*
Manuscript ID	JAERO-17-0747.R3
Manuscript Type:	Original article
Date Submitted by the Author:	03-Mar-2018

Complete List of Authors:	Rezaei, Mohsen; Shiraz University, School of Mechanical Engineering Fazelzadeh, S.Ahmad; Shiraz University, Mechanical Eng. Mazidi, Abbas; Yazd University, Mechanical Engineering Khodaparast, Hamid Haddad; Swansea University

Keywords:	Uncertainty, Flutter, Aircraft wing, Thrust force, Fuzzy method, Non-Probabilistic

Abstract:	In this study, flutter uncertainty analysis of an aircraft wing subjected to a thrust force is investigated using fuzzy method. The linear wing model contains bending and torsional flexibility and the engine is considered as a rigid external mass with thrust force. Peters' unsteady thin airfoil theory is used to model the aerodynamic loading. The aeroelastic governing equations are derived based on Hamilton's principle and converted to a set of ordinary differential equations using Galerkin method. In the flutter analysis, it is assumed that the wing static deflections do not have influence on the results. The wing bending and torsional rigidity, aerodynamic lift curve slope and air density are considered as uncertain parameters and modelled as triangle and trapezium membership functions. The eigenvalue problem with fuzzy input parameters is solved using fuzzy Taylor expansion method and a sensitivity analysis is performed. Also, the upper and lower bounds of flutter region at different α-cuts are extracted. Results show that this method is a low-cost method with reasonable accuracy to estimate the flutter speed and frequency in the presence of uncertainties.

Fuzzy uncertainty analysis in the flutter boundary of an aircraft wing subjected to a thrust force

M. Rezaei[1], S. A. Fazelzadeh[1]*, A. Mazidi[2], H. H. Khodaparast[3]

[1]School of Mechanical Engineering, Shiraz University, Shiraz, Iran

[2]School of Mechanical Engineering, Yazd University, Yazd, Iran

[3]College of Engineering, Swansea University, Swansea, United Kingdom

ABSTRACT

In this study, flutter uncertainty analysis of an aircraft wing subjected to a thrust force is investigated using fuzzy method. The linear wing model contains bending and torsional flexibility and the engine is considered as a rigid external mass with thrust force. Peters' unsteady thin airfoil theory is used to model the aerodynamic loading. The aeroelastic governing equations are derived based on Hamilton's principle and converted to a set of ordinary differential equations using Galerkin method. In the flutter analysis, it is assumed that the wing static deflections do not have influence on the results. The wing bending and torsional rigidity, aerodynamic lift curve slope and air density are considered as uncertain parameters and modelled as triangle and trapezium membership functions. The eigenvalue problem with fuzzy input parameters is solved using fuzzy Taylor expansion method and a sensitivity analysis is performed. Also, the upper and lower bounds of flutter region at different α-cuts are extracted. Results show that this method is a low-cost method with reasonable accuracy to estimate the flutter speed and frequency in the presence of uncertainties.

*Corresponding author. Tel.: +98 7136133238; fax: +98 7136473511.
E-mail address: Fazelzad@shirazu.ac.ir (S. A. Fazelzadeh).

KEYWORDS: *Uncertainty; Flutter; Aircraft wing; Thrust force; Fuzzy method, Non-Probabilistic.*

NOMENCLATURE

A, B - Eigenvalue problem matrixes

$\underset{\sim}{A}$ - Finite state pressure loading coefficient

C_{L_θ} – Lift curve slope coefficient

E - Elastic modulus

G - Shear modulus

EI_n – Bending rigidity nominal value

GJ_n – Torsional rigidity nominal value

H - Heaviside function

I - Wing cross-sectional moment of inertia

J - Wing cross-sectional polar moment of inertia

K_e - Engine mass radius of gyration

L - Aerodynamic lift

M - Aerodynamic moment

M_e - Engine mass

P - Dimensionless thrust force

P_e - Engine thrust force

SN - Sensitivity of non-dimension parameters

T_e - Engine kinetic energy

T_w - Wing kinetic energy

U - Airstream velocity

U_s - Wing strain energy

W_a - Work done by aerodynamic forces

W_f - Work done by thrust forces

X_e, Y_e, Z_e - Dimensionless engine location

b - Wing semichord

$\underset{\sim}{c}$ - Finite state pressure loading coefficient

g - Modal damping

l - Wing length

$m_{(x)}$ - Wing mass per unit length

n - Number of modes

n_w - Number of bending modes

n_θ - Number of torsional modes

n_λ - Number of induced flow states

q_j - j^{th} eigenvector corresponding to λ_j

v - Dimensionless air speed

v_f - Dimensionless flutter speed

w - Wing bending deflection

x_e, y_e, z_e - engine location

λ_j - j^{th} eigenvalue

θ – Wing torsion deflection

ρ – Air density

$\tilde{\zeta}$ - Fuzzy uncertain parameters

1 INTRODUCTION

Loading high thrust engines on aircraft wings is the common configuration of modern civil aircraft. The evaluation of the flutter instability for such aircraft wings has been a challenge for aeronautical engineering for many years [1-3]. Hodges et al. [4] investigated the effect of thrust on the flutter of a high-aspect-ratio wing. They showed that high thrust force may lead to the wing instability at very low air speeds. Fazelzadeh et al. [5-6] presented a deterministic model for bending torsional flutter characteristic of a wing under follower force. They have studied the flutter of an aircraft wing carrying a powered engine and indicated the importance of the engine thrust on the flutter speed and frequency.

Aeroelasticity is an integral and major component of aircraft engineering design and manufacturing. The key airworthiness requirements for aircraft are all based on aeroelastic effects. Most of the current industry practices are based on deterministic aeroelastic analysis. However, aircraft operates in an uncertain environment. Moreover, the structural parameters of aircraft cannot be considered deterministic due to manufacturing variabilities. To this end, the use of non-deterministic aeroelastic analysis is of paramount importance. Generally, two approaches namely probabilistic and non-probabilistic are available for uncertainty modelling. Non-probabilistic methods have been preferred in recent years due to difficulty in obtaining probabilistic distribution of uncertain parameters. This difficulty is mainly due to lack of data that could be used to determine the statistical distribution of uncertain parameters. In this regard, Rao and Berke [7] investigated the modelling of uncertain structural systems using interval analysis. They represented each uncertain input parameter as an interval variable. Muhanna and Mullen [8] presented a non-traditional uncertainty treatment for mechanics problems. In their work uncertainties are introduced as bounded possible values (intervals). Qiu and Wang [9] presented the non-probabilistic interval analysis method for the dynamical response of structures with uncertain-but-bounded parameters. Qiu [10] used convex models and interval analysis method to predict the effect of uncertain-but-bounded parameters on the buckling of composite structures. Muhanna et al. [11] presented an interval approach for the treatment of parameter uncertainty for linear static problems of mechanics. They combined interval analysis and finite element methods to analyse the system response due to uncertain stiffness and loading. Xiaojun and Zhiping [12] studied the influences of uncertainty parameters on the flutter speed of a wing. The uncertain parameters were described by interval numbers. They found the upper and lower bound of flutter speed using first order Taylor series expansion. They have only studied the structural parameters and other parameters such as geometric, aerodynamic and loading have not been mentioned in their work. Yun and Hun [13] investigated the problem of robust stability of a 2-D nonlinear aeroelastic system with structural and aerodynamic uncertainties using μ-method and value set approach.

Sarkar et al. [14] studied the effect of system parametric uncertainty on the stall flutter bifurcation behaviour of a pitching airfoil. Khodaparast et al. [15] investigated the problem of linear flutter analysis in the presence of structural uncertainty. Danowsky et al. [16] investigated three different methods for uncertainty analysis of (Monte Carlo, DOE/ RSM, and analysis) an Aeroelastic wing model. Badcock et al. [17] reviewed the use of eigenvalue stability analysis of very large dimension aeroelastic numerical models arising from the exploitation of computational fluid dynamics. Yang et al. [18] proposed an interval based method for dynamic analysis of structures with uncertain parameters using Laplace transform. Muscolino and Sofi [19] proposed a stochastic analysis of linear structures, with slight variations of the structural parameters, subjected to zero-mean Gaussian random excitations. The uncertain-but-bounded parameters are modelled as *interval variables*. Gu et al. [20] formulated robust flutter analysis as a nonlinear programming problem. In their work, the worst-case parametric perturbations and the robust flutter solution are solved by genetic algorithm optimization approach. Song et al. [21] presented an uncertain aeroelastic model of the 3-dimensional advanced aircraft wing system operating in subsonic compressible flow field and controlled its vibration using sliding mode observer. Sofi et al. [22] evaluated the lower and upper bound of the natural frequencies of structures with uncertain but bounded parameters. They applied the improved interval analysis via extra unitary interval (EUI). Mannini and Bartoli [23] presented a method to approach flutter instability in a probabilistic way and calculated the critical wind speed, starting from the probability distribution of the flutter derivatives. Abbas and Morgenthal [24] used a probabilistic flutter analysis utilizing a meta-modelling technique to evaluate the effect of parameter uncertainty on flutter speed. Wu and Livune [25] studied the flutter of an AGARD wing in the presence of aerodynamic and structural uncertainties by a newly developed Monte Carlo simulation. Lokatt [26] presented a method for efficient flutter analysis of aeroelastic systems including modelling uncertainties. The aerodynamic model is approximated by a piece-wise continuous rational polynomial function. Huan et al. developed a framework of effective robust design optimization to design the high-performance transonic high lift natural-laminar-flow (NLF) airfoil at low Reynolds numbers [27]. They used polynomial chaos expansion (PCE) method for uncertainty quantification and show that this method has less computational cost when compared to Monte Carlo simulation.

Some researchers used fuzzy approach for uncertainty modelling and propagation. This method is a non-probabilistic method and computationally is low-cost compared to probabilistic methods [28]. Chiang et al. [29] studied the response of structures with uncertainty properties such as mass, stiffness and damping. They modeled system with fuzzy and random uncertainties. Massa et al. [30] presented a fuzzy methodology to calculate the eigenvector and eigenvalue of a mechanical structure defined by imprecise parameters. They described material and geometric parameters as imprecise fuzzy numbers. Damping and other non-conservative parameters were not considered in their work. De Gersem et al. [31] examined the interval and fuzzy finite element method for the eigenvalue and frequency response function analysis of structures with uncertain parameters. They combined non-probabilistic methods with the component mode synthesis technique in order to reduce the calculation time. Tartaruga et al. [32] used probabilistic and non-probabilistic approaches to predict the flutter dynamic pressure of a semi-span super-sonic wind-tunnel model. Khodaparast et al. [33] presented the application of the fuzzy finite element model updating to the DLR AIRMOD structure. In their work, the histogram of measured data attributed to the uncertainty of the structural components in terms of mass and stiffness are utilised to obtain the membership function of the chosen fuzzy outputs and to determine the updated membership function of the uncertain input parameters represented by fuzzy variables.

According to the best of the authors' knowledge, in the pertinent literature, aeroelastic analysis of wings subjected to thrust force under all type of uncertainties containing structural and aerodynamic design parameters using fuzzy approach have not yet been presented. This study intends to fill the gap in the knowledge associated with this problem. In this paper, parameter sensitivity with various order of magnitudes is carried out for different airspeeds. Furthermore, modal damping vs airspeed diagrams, at different α-cuts, are presented.

2 PROBLEM STATEMENT

The aircraft wing subjected to a powered engine, shown in Fig.1, is considered. The undeformed shape of the wing is shown in Fig.1 (a) and the typical section of the wing is shown in Fig.1 (b). The distance of the engine from the wing root is determined by (x_e , y_e ,z_e). AE, AC, c_{gw} and c_{gs} are the wing elastic axis, the wing aerodynamic centre, the wing centre of gravity and the engine centre of gravity, respectively.

The structural model of the wing contains bending and torsional flexibility. After the wing deformation, the shear center of the cross-section located at x is displaced by an amount of w in z direction. Additionally, the angle of twist of the cross-section changes to θ about the x axis. Aerodynamic pressure loading based on Finite State unsteady thin airfoil theory is also applied on this model. Torsional and bending rigidity, lift curve slope and air density are considered as fuzzy uncertain parameters, in the model. These uncertain parameters are modelled as fuzzy membership functions.

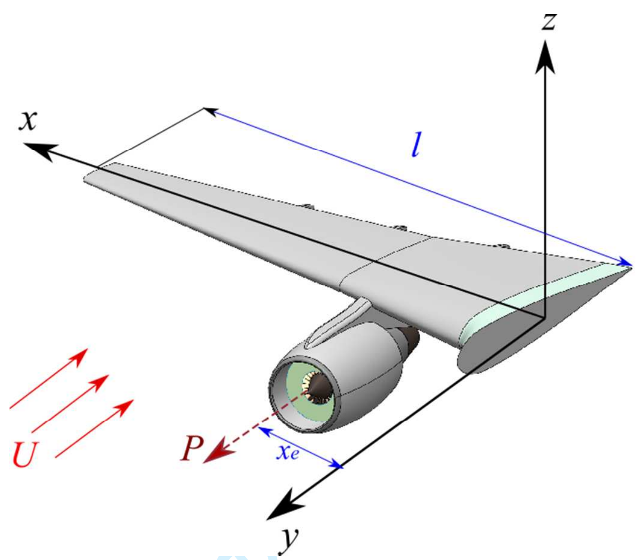

(a)

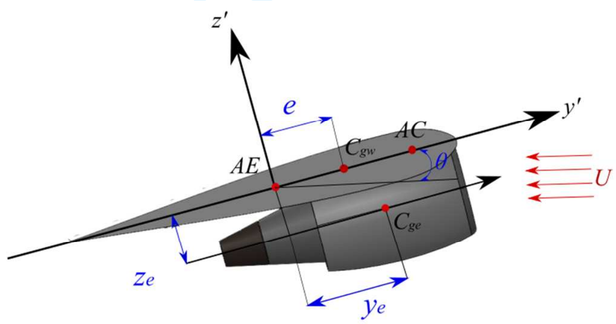

(b)

Figure 1. (a) Aircraft wing subjected to a thrust load, (b) the wing typical section.

3 GOVERNING EQUATION

The equations of motion and boundary conditions are developed by Hamilton's principle as

$$\int_{t_1}^{t_2}\left(\delta U_s - \delta T_e - \delta T_w - \delta W_a - \delta W_f\right)dt = 0 \quad \delta w = \delta\theta = 0 \;\; at \;\; t = t_1 = t_2 \tag{1}$$

where U and T_w are strain and kinetic energy of the wing and T_e is the kinetic energy of the engine. W_f and W_a are works done by thrust force and aerodynamic forces, respectively. The final equations of motion are derived by extending the above equation [5].

$$\begin{aligned}\delta w:\ & m_{(x)}\ddot{w}+m_{(x)}y_\theta\ddot{\theta}+EIw''''+M_e\left(-z_e{}^2\ddot{w}''+y_e\,\ddot{\theta}+\ddot{w}\right)\delta_D\left(x-x_e\right)\\ & +P_e\left(x_e-x\right)H\left(x_e-x\right)\theta''-2P\theta'=L\left(x,t\right)\end{aligned} \tag{2}$$

$$\begin{aligned}\delta\theta:\ & m_{(x)}k_{EA}^2\ddot{\theta}+m_{(x)}y_\theta\ddot{w}-GJ\theta''+M_e\left(\left(z_e{}^2+y_e{}^2+K_e^2\right)\ddot{\theta}+y_e\ddot{w}\right)\delta_D\left(x-x_e\right)\\ & +P_e\left(x_e-x\right)H\left(x_e-x\right)w''=M\left(x,t\right)\end{aligned} \tag{3}$$

Peters et al. finite state unsteady aerodynamic model is used to simulate aerodynamic forces [34].

$$L\left(x,t\right)=-\pi\rho b^2\left[\ddot{w}-U\dot{\theta}+ba\ddot{\theta}\right]+C_{L_\theta}\rho Ub\left[-\dot{w}+U\theta-ba\dot{\theta}+\frac{b}{2}\left(\frac{C_{L_\theta}}{\pi}-1\right)\dot{\theta}-\lambda_0\left(t\right)\right] \tag{4}$$

$$\begin{aligned}M\left(x,t\right)&==-\pi\rho b^3\left[\frac{1}{2}\left(\frac{C_{L_\theta}}{\pi}-1\right)U\dot{\theta}-Ua\dot{\theta}+a\ddot{w}+b(\frac{1}{8}+a^2)\ddot{\theta}\right]\\ &+C_{L_\theta}\rho Ub^2\left(a+\frac{1}{2}\right)\left[U\theta-\dot{w}-ba\dot{\theta}+\frac{b}{2}\left(\frac{C_{L_\theta}}{\pi}-1\right)\dot{\theta}-\lambda_0\left(t\right)\right]\end{aligned} \tag{5}$$

where $\lambda_0=\sum_{n=1}^{\infty}b_n\lambda_n$ is the induced flow velocity, calculated through a system of N first order coupled differential equations [35].

4 SOLUTION APPROACH FOR DETERMINISTIC MODEL

Due to the complexity of the governing equations, an approximate solution methodology should be used to solve them. Galerkin method is a simple and accurate choice for solving these equations. In this method, the wing bending and torsion are expressed as the following series

$$w\left(x,t\right)=\sum_{j=1}^{n_w}W_j\left(x\right)\varphi_j\left(t\right)\quad,\quad\theta\left(x,t\right)=\sum_{n=1}^{n_\theta}\Theta_j\left(x\right)\psi_j\left(t\right) \tag{6}$$

where $\varphi_j(t)$ and $\psi_j(t)$ are the time dependent modal coordinates and $W_j(x)$ and $\Theta_j(x)$ are the bending and torsional trial functions. n_w and n_θ are the number of trial functions used for representation of w and q, respectively.

By using suitable family of orthogonal functions for w and q, substituting Eq.7 in Eqs.2 and 3, and applying the Galerkin procedure results in discrete equations of motion as follows::

$$[M]\{\ddot{q}\}+([C]+U[G])\{\dot{q}\}+([K]+U[L]+U^2[H])\{q\}=0 \tag{7}$$

where [M] is mass matrix, [C] is damping matrix, U [G] is damping matrix due to aeroelastic terms, [K] is structural stiffness and $(U[L]+U^2[H])$ is aeroelastic stiffness matrix due to circularity forces. The final state space form of discrete governing equations can be developed as:

$$[A]\{\dot{q}\}=[B]\{q\} \tag{8}$$

After solving above eigenvalue problem, the modal damping and frequency at different airspeeds are obtained.

5 MODELING UNCERTAINTY WITH FUZZY APPROACH

In this section, the uncertain parameters are modelled using fuzzy expansion approach [30]. The eigenvalue problem of Eq.8 can be described as:

$$([B]-\lambda[A])\{q\}=0 \qquad j=1,2,\ldots,n \ \ \& \ \ n=2n_w+2n_\theta+ \tag{9}$$

where λ_j is the j^{th} eigenvalue, q_j is the j^{th} eigenvector, n_w is the number of bending modes, n_θ is the number of torsional modes and n_λ *is* the number of induced flow states. It is assumed that the bending and torsional rigidity, lift curve slope and air density are not deterministic parameters. Because these parameters are imprecise they are modelled by fuzzy numbers.

Each fuzzy value $\tilde{\zeta}$ is represented as a fuzzy triangle and trapezium membership function, showing respectively in figure 2(a) and (b) and as:

$$\tilde{\zeta} = \xi_c + \Delta\tilde{\zeta} \tag{10}$$

ζ_c is a nominal or crisp value and $\Delta\zeta^{\alpha}$ is the variation associated to each α-cut. According to Fig.2, an α-cut of the membership function is the set of all ζ such that $\mu(\zeta)$ is greater than or equal to α. For each α-cut

$$\tilde{\zeta} = \xi_c + \left[\underline{\Delta\zeta^{\alpha}};\overline{\Delta\zeta^{\alpha}}\right] \tag{11}$$

In which $\underline{\zeta^{\alpha}}$ and $\overline{\zeta^{\alpha}}$ are minimum and maximum values of fuzzy parameter $\tilde{\zeta}$ for a given α-cut, respectively. The membership function is discretized by different intervals which are linked to an α-cut ranging from 0 to 1 [23].

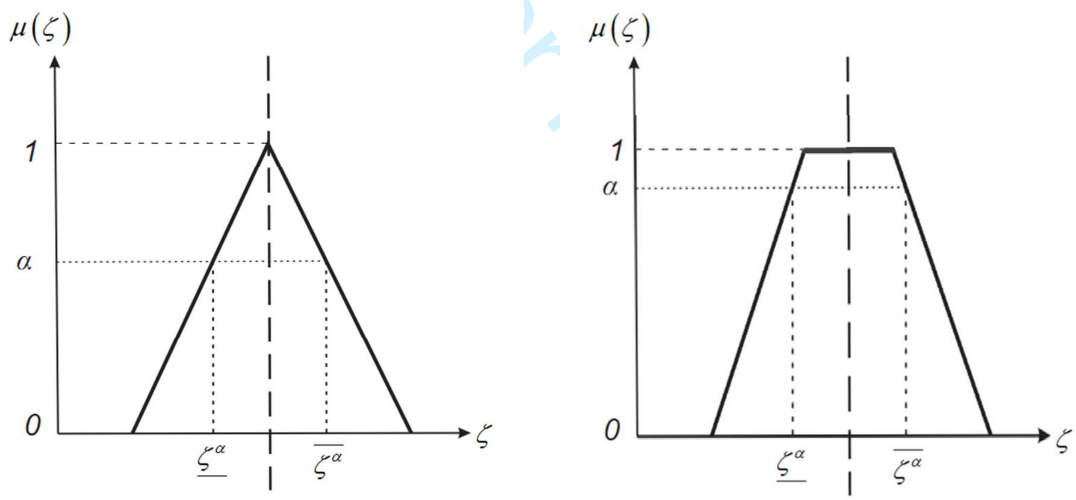

(a) **(b)**

Figure 2. Fuzzy membership functions and (a) triangle (b) trapezium.

In the presence of *m* fuzzy parameters, the eigenvalue problem can be rewritten as:

$$\left[B\left(\tilde{\zeta}_1,\tilde{\zeta}_2,\ldots,\tilde{\zeta}_m\right)\right]\left\{\tilde{q}_j\right\} = \tilde{\lambda}_j\left[A\left(\tilde{\zeta}_1,\tilde{\zeta}_2,\ldots,\tilde{\zeta}_m\right)\right]\left\{\tilde{q}_j\right\} \tag{12}$$

α-cut method is an approach for solving this type of eigenvalue problems [36]. In this method, the fuzzy membership function is discretized to different intervals using α-level cut concept. For each α-level cut the eigenvalue problem is solved with the Neumann series of first order perturbation method.

In this paper, to solve the flutter uncertain problem, the Taylor series expansion is used to determine the crisp value (TSEC). TSEC is a method that evaluates the derivatives of crisp values of the eigenvalues and eigenvectors with respect to fuzzy parameters. In this method, the fuzzy eigenvalues and eigenvectors are determined as:

$$\tilde{\lambda}_j^{\alpha} = \lambda_{j_c} + \sum_{j=1}^{n} \frac{\partial \lambda_j}{\partial \zeta_i} \Delta \tilde{\zeta}_i^{\alpha}$$
$$\left\{\tilde{q}_j^{\alpha}\right\} = \left\{q_{j_c}\right\} + \sum_{j=1}^{n} \frac{\partial \left\{q_j\right\}}{\partial \zeta_i} \Delta \tilde{\zeta}_i^{\alpha} \tag{13}$$

where $\Delta\tilde{\zeta}_i^{\alpha} = \left[\underline{\Delta\zeta^{\alpha}}; \overline{\Delta\zeta^{\alpha}}\right]$. The value of $\frac{\partial \lambda_j}{\partial \zeta_i}$ can be determined as [28]:

$$\frac{\partial \lambda_j}{\partial \zeta_i} = \left\{q_{j_c}^T\right\} \left(\frac{\partial [B]}{\partial \zeta_i} - \lambda_j \frac{\partial [A]}{\partial \zeta_i} \right) \left\{q_{j_c}\right\} \tag{14}$$

The above equation also demonstrates the sensitivity of eigenvalues with respect to parameter ζ_i. For modelling the uncertainty in the flutter problem, the fuzzy parameter should be determined, primarily. $\tilde{EI}, \tilde{GJ}, \tilde{\rho}, \tilde{C}_{L_\theta}, \tilde{P}$ are considered as uncertain parameters of the wing. The bending and torsional rigidity $\tilde{EI}$ and $\tilde{GJ}$ are structural uncertain parameters and the air density $\tilde{\rho}$ is an aerodynamic uncertain parameter which varies with the aircraft flight altitude. Also, the wing lift curve slope $\tilde{C}_{L_\theta}$ and the engine thrust are other uncertain parameters. These parameters are modelled using the triangle and trapezium fuzzy membership function as shown in Fig.2. After modelling the uncertain parameters, the final equation for fuzzy eigenvalue problem is determined as:

$$\tilde{\lambda}_j^{\alpha} = \lambda_{j_c} + \frac{\partial \lambda_j}{\partial (EI)} \Delta\left(\tilde{EI}\right)^{\alpha} + \frac{\partial \lambda_j}{\partial (GJ)} \Delta\left(\tilde{GJ}\right)^{\alpha} + \frac{\partial \lambda_j}{\partial \rho} \Delta\tilde{\rho}^{\alpha} + \frac{\partial \lambda_j}{\partial C_{L_\theta}} \Delta\tilde{C}_{L_\theta}^{\ \alpha} \tag{15}$$

The mentioned procedure is illustrated in Fig.3.

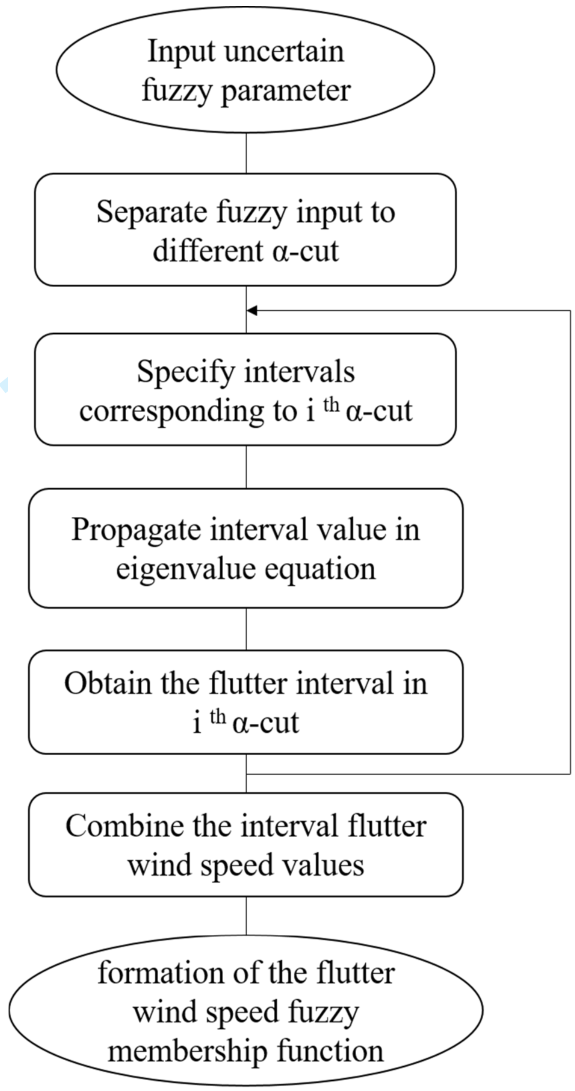

Figure 3. The Flowchart of Fuzzy interval Method

6 NUMERICAL RESULTS

6.1 Validation of Deterministic Problem

Related data for the wing which is used here is given in Table 1. As stated in the previous section, the solution to deterministic problem through the Galerkin method is sought by using a numerical integration scheme. Clearly, increasing the number of modes assure the accuracy of results. But, in addition to this fact the computational effort should be kept from being overly burdensome. So, one should use optimized number of modes to get both accuracy and ease of computing together. In this work, the number of modes is increased until convergence is obtained. Therefore, to get both accuracy and ease of computing together, two modes are selected for bending and torsion. By considering two bending modes in *w* direction, two torsion modes and two aerodynamic states in Galerkin procedure, Eqs.2 and 3 will be converted to a set of first order coupled ordinary differential equations.

Table 1: The wing model characteristics [4].

Parameters	Value
Wing Length	16 m
Semi-chord	0.5 m
Bending rigidity	2e4 N.m^2
Torsional rigidity	2e3 N.m^2
Mass per unit length	0.75 Kg/m
Wing moment of inertia	0.1 Kg.m

The following dimensionless parameters are used in this study:

$$P=\frac{P_e\ell^2}{\sqrt{GJ_n\,EI_n}}\;,v=\frac{U}{b\,\omega_\theta},X_e=\frac{x_e}{\ell},Y_e=\frac{y_e}{b},Z_e=\frac{z_e}{b}$$
$$SN_{EI}=\frac{\partial\left(\lambda_j/\lambda_{jn}\right)}{\partial\left(EI/EI_n\right)},SN_{GJ}=\frac{\partial\left(\lambda_j/\lambda_{jn}\right)}{\partial\left(GJ/GJ_n\right)},SN_{C_{L\theta}}=\frac{\partial\left(\lambda_j/\lambda_{jn}\right)}{\partial\left(C_{L\theta}/C_{L\theta n}\right)},SN_{\rho}=\frac{\partial\left(\lambda_j/\lambda_{jn}\right)}{\partial\left(\rho/\rho_n\right)} \tag{16}$$

It should be noted that static deflections of the wing at severe conditions of non-dimensional parameters used for the paper, remain within the linear model assumption. As shown in Fig. 4, flutter boundary results are compared with previous published studies, such as Fazelzadeh et al. [5] and Hodges et al. [4] and good agreement is observed. Only, at high values of the thrust some differences take place between the results and those obtained by Hodges et al. This may come from the fact that the Galerkin method is used here instead of the finite element method, which was used by them in solution procedure. This validation is performed to determine the accuracy of the current aeroelastic governing equations and the solution methodology in the presence of engine thrust.

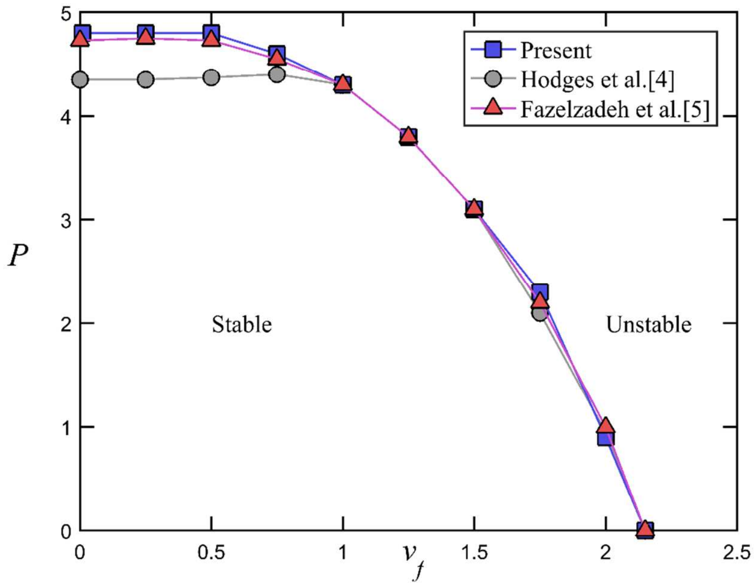

Figure 4. Flutter boundary of a clean wing subjected to thrust force.

Furthermore, the flutter boundary of the deterministic model of a wing with an external mass also is compared with previous published papers and good agreement is observed.

Table 2: Deterministic flutter speed and frequency comparison

Refrence	Flutter Speed(m/s)	Error (%)	Frequency Flutter(Hz)	Error(%)
Goland and Luke[1]	494.1	-	11.25	-
Gern and Liberscu[3]	493.6	-0.1	12.02	6.84
Fazelzadeh et al [5].	493.4	-0.14	12.02	6.84
Borello et al.[37]	508.2	2.85	11.55	2.67
Present	494.3	0.04	11.33	0.07

6.2 Investigating Flutter under Uncertainty

In this section, the flutter analysis with uncertain parameters is investigated. The values of uncertain parameters are specified in Table 3 and Table 4.

Table 3: Uncertain fuzzy parameters (Triangle membership function).

Parameters	Minimum Value	Crisp Value	Maximum Value	Percentage of Variation
Bending Rigidity	19000	20000	21000	±5%
Torsional Rigidity	1900	2000	2100	±5%
Air Density	0.0845	0.0889	0.0933	±5%
Lift Curve Slope	5.3058	5.5851	5.8643	±5%

Table 4: Uncertain fuzzy parameters (Trapezium membership function).

Parameters	Minimum Value	Minimum Middle value	Crisp Value	Maximum Middle value	Maximum Value	Percentage of Variation
Bending Rigidity	19000	19800	20000	20200	21000	±5%
Torsional Rigidity	1900	1980	2000	2020	2100	±5%
Air Density	0.0845	0.088	0.0889	0.0898	0.0933	±5%
Lift Curve Slope	5.3058	5.5292	5.5851	5.6409	5.8643	±5%

The sensitivity analysis of the system eigenvalues with respect to above parameters (EI, CJ, ρ and C_{L_θ}) at different air speeds with dimensionless trust force P=4.5 is shown in Fig.5. Because the order of sensitivity magnitudes is very different, the y axis is shown in logarithmic scale. This figure shows that the sensitivity to air density and lift curve slope is much larger than the sensitivity to geometric and structural parameters. As expected, this result shows that the air density and lift curve slope have significant impact on the wing flutter phenomenon.

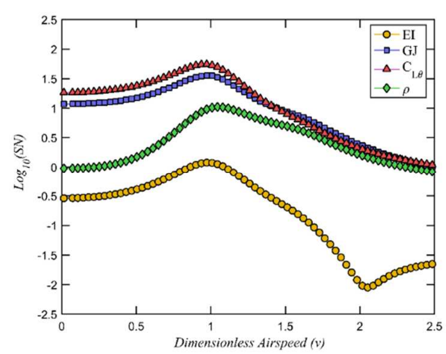

Figure 5. Dimensionless sensitivity vs dimensionless airspeed at P=4.5.

Since the parameter sensitivity analysis at the flutter boundary is more important, the dimensionless sensitivity with respect to above parameters (*EI*, *GJ*, ρ and C_{L_θ}) near flutter speed for different dimensionless thrust forces is shown in Fig.6 in logarithmic scale. The figure shows that the variation of bending rigidity has less effect on the wing flutter speed compare to the other parameters. The sensitivity analysis show that the variation of lift curve slope has significant effect on the flutter speed. With increasing thrust force, the sensitivity of studied parameters increases. In the absence of thrust force the aerodynamic uncertainty has great impact on flutter, but in the presence of thrust force, impact of the structural uncertainty on flutter boundary grows.

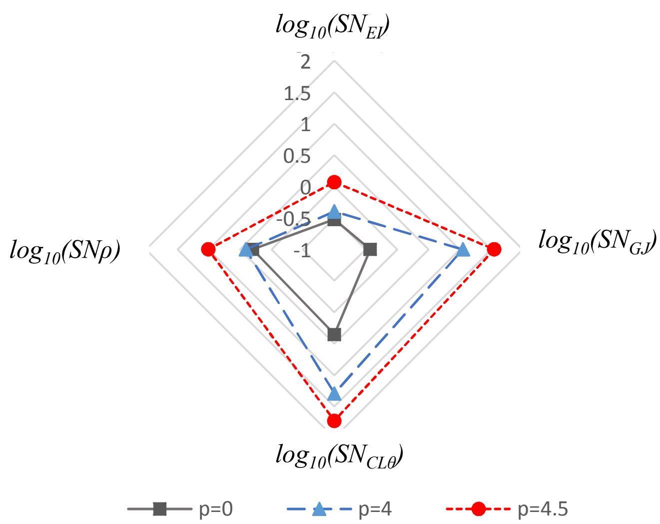

Figure 6. Dimensionless sensitivity at flutter speed for different dimensionless thrust forces.

The modal damping versus air speed for uncertain triangle fuzzy parameters at α-cut=0 (largest interval) and α-cut=0.5 for different dimensionless thrust force P is shown in Fig.7. This figure shows the modal damping of the wing first bending mode and first torsion mode.

In Fig.7 (a) and (b) the effect of thrust force at zero α-cut is illustrated. It can be seen that increasing the thrust force will decrease the flutter speed. Furthermore, increasing the thrust force tightens the flutter speed range due to uncertainties. These results are repeated for α =0.5 that is shown in Fig .7 (c) and (d) and the same conclusion is also drawn in this case.

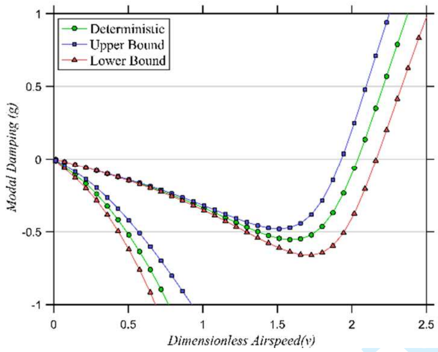

(a)

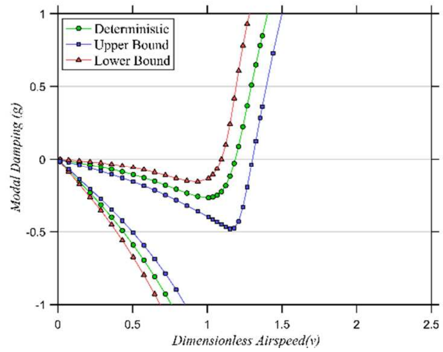

(b)

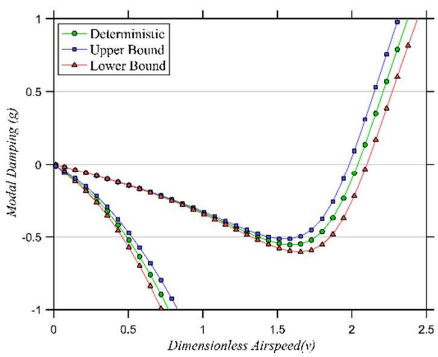

(c)

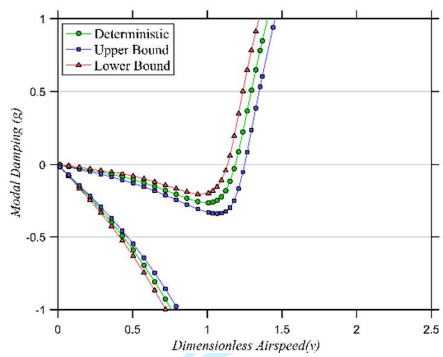

(d)

Figure 7. Modal damping vs dimensionless airspeed for different thrust forces

(a) α-cut=0, P=0; (b) α-cut=0, P=4; (c)α-cut=0.5, P=0; (d)α-cut=0.5, P=4.

The first bending mode modal damping vs airspeed at different α-cuts and also different dimensionless thrust forces is shown in Fig.8. In this figure, the flutter boundary range can be seen in a triangle fuzzy mountain shape. For each value of the thrust force and in every α-cut section, the upper and lower bounds of the flutter speed can be extracted from this figure.

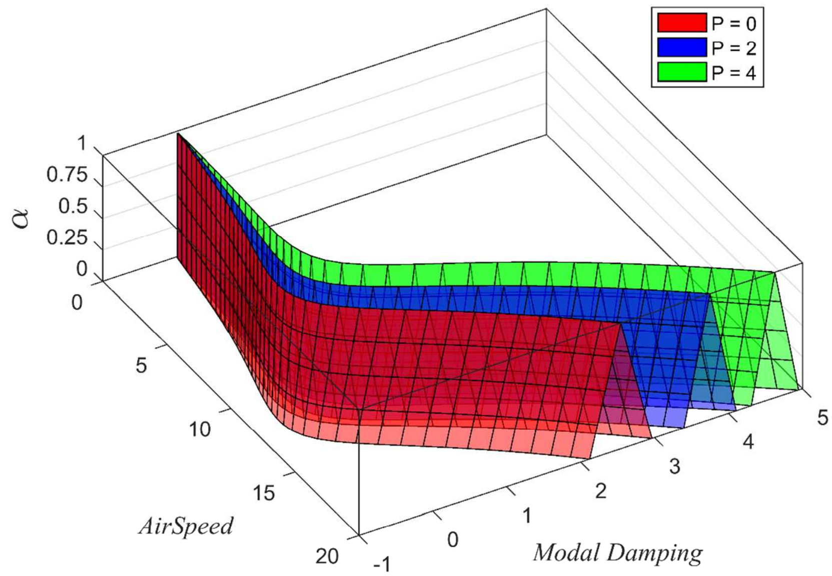

Figure 8.Modal damping vs airspeed in different α-cuts at P=0, 2, 4.

The dimensionless flutter speed versus thrust force for uncertain triangle fuzzy parameters for different α-cut is shown in Fig.9. The α varies between 0 (largest interval Fig.9 (a)) and 1 (deterministic model Fig 9.(d)). It can be seen that increasing the thrust force and α will tighten the flutter region.

The 3D figure of the flutter speed vs thrust force at different α-cuts is shown in Fig.10. In this figure, the flutter region can be seen as a fuzzy mountain shape. For each value of α, the upper and lower bounds of flutter stability region can be extracted from this figure. As it is expected, the flutter region is similar to input membership functions.

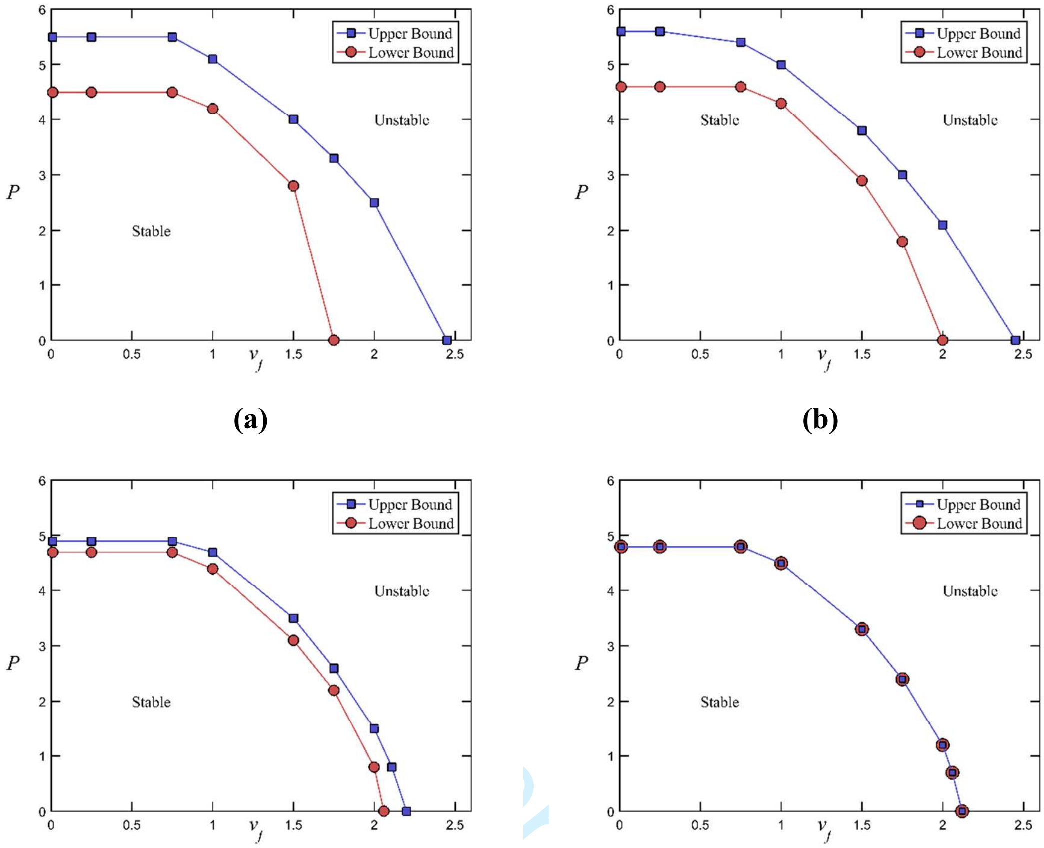

(a) (b)

(c) (d)

Figure 9. Thrust force vs flutter speed with triangle membership functions for (a) α-cut=0; (b) α-cut=0.4; (c) α-cut=0.8, (d)α-cut=1.

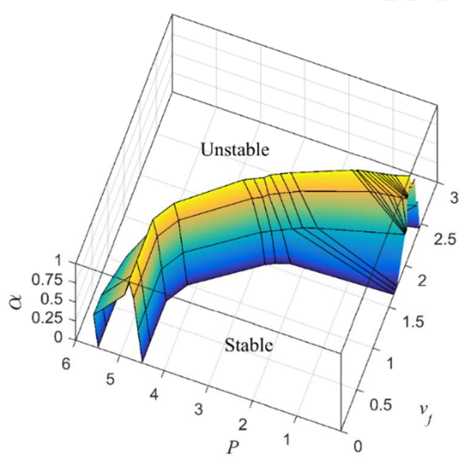

Figure 10. Thrust force vs flutter speed in different α-cuts for triangle membership function.

Fig.11 and Fig.12 indicates the dimensionless flutter speed versus thrust force for different α-cuts in the case that uncertain parameters have been chosen as trapezium fuzzy functions. As expected the flutter region in Fig. 12 is similar to input membership functions and for each value of α, the upper and lower bounds of flutter stability region can be extracted from this figure.

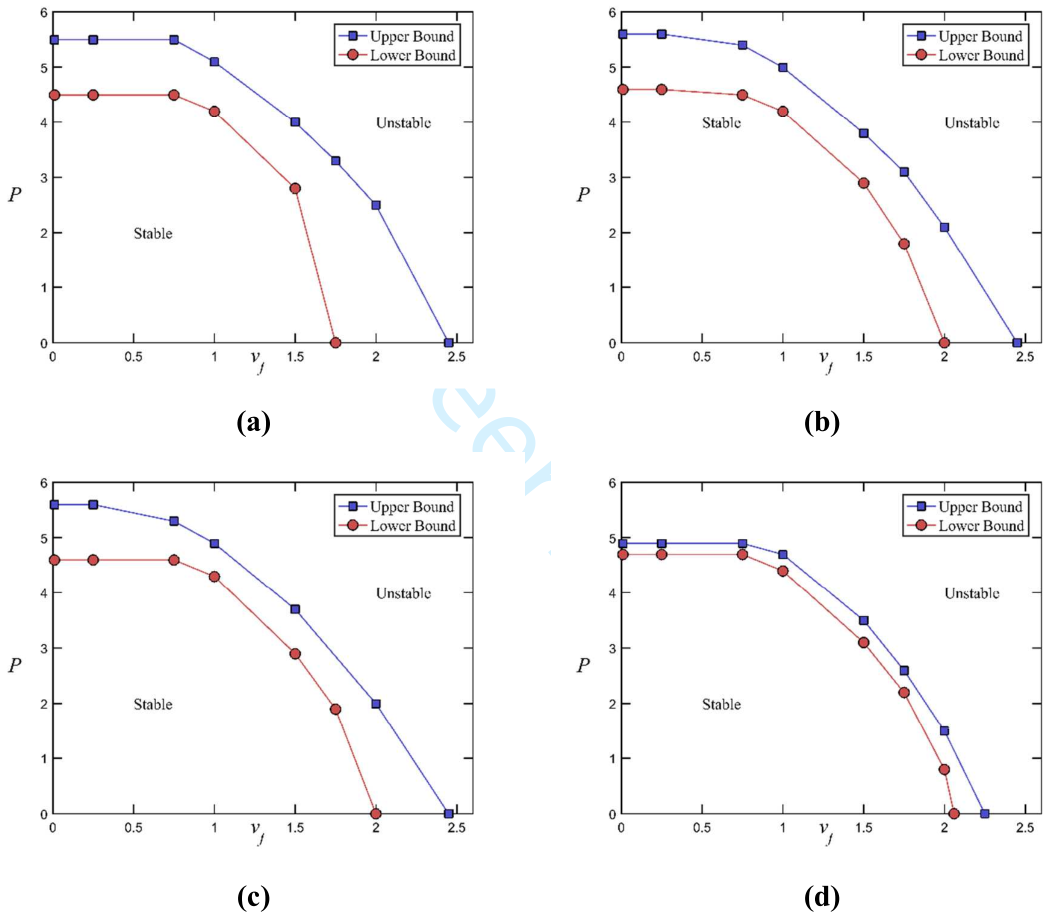

Figure 11. Thrust force vs flutter speed trapezium membership function (a) α-cut=0; (b) α-cut=0.4; (c) α-cut=0.6, (d) α-cut=1.

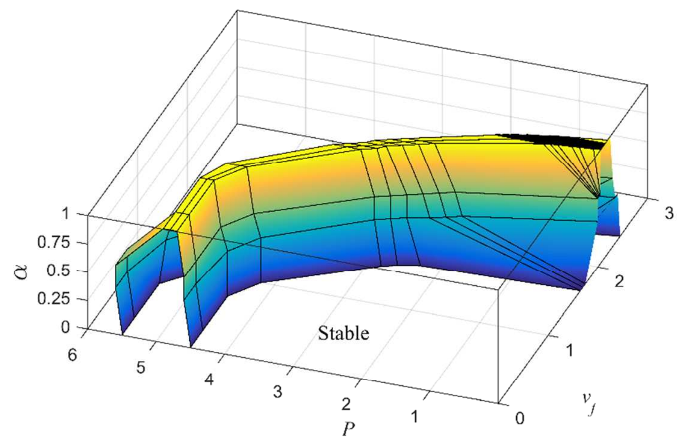

Figure 12. Thrust force vs flutter speed in different α-cuts for trapezium membership functions.

Fig.13 demonstrates the effects of each parameter uncertainty with triangle membership function on the stability region of the wing. Results show that although by increasing the thrust force, effects of the wing bending rigidity increases, but in general the impact of bending rigidity uncertainty on flutter boundary is low. Fig.13 (b) shows that uncertainty in the wing torsional rigidity can considerably influence the flutter boundary for all thrust forces. Furthermore, it can be seen in Fig.13 (c) and Fig.13 (d) that increasing the thrust force will decrease the effects of lift curve slope and air density uncertainties on the flutter boundary. It means that changes in altitude and wind conditions which leads to changes in aerodynamic parameters at low thrust conditions may change the flutter boundary, dramatically.

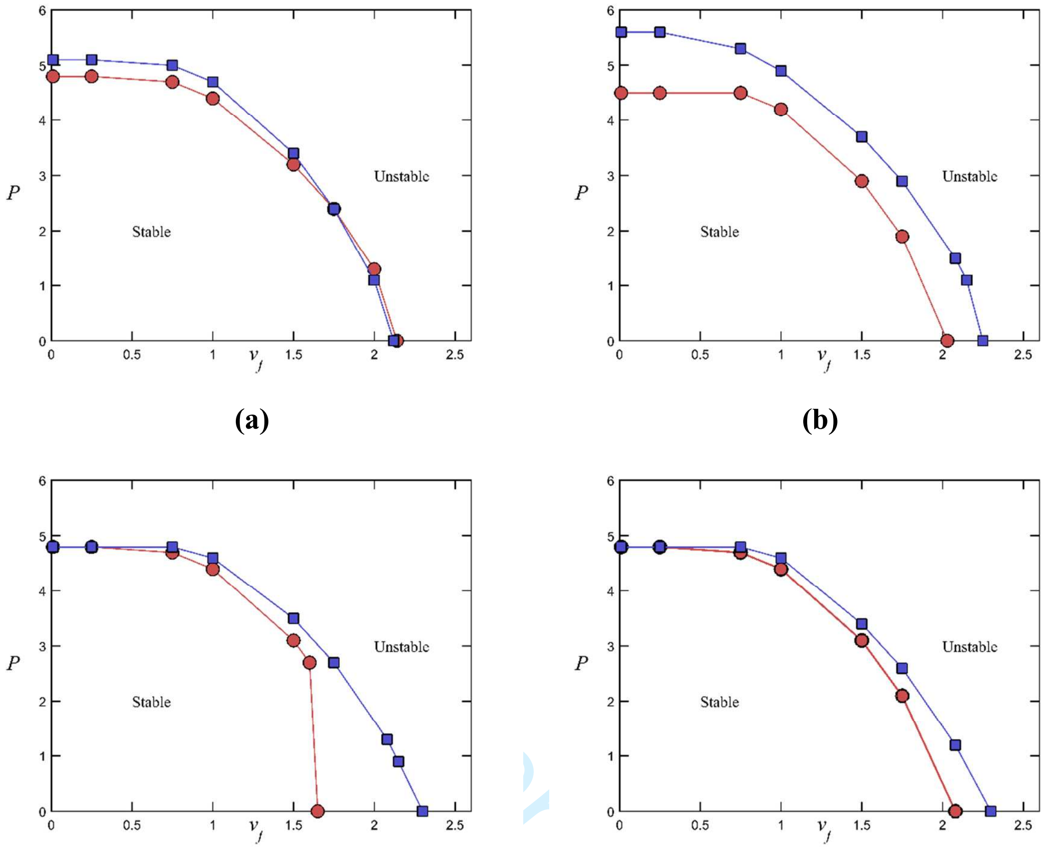

(a) (b)

(c) (d)

Figure 13. Thrust force vs Flutter speed in α-cut= 0 for uncertain parameter (a) *EI* ; (b) *GJ*; (c) C_{L_θ} ; (d) *ρ*.

The dimensionless flutter speed versus dimensionless engine position with uncertain triangle fuzzy parameters for different α-cut is shown in Fig.14. In this simulation α varies between 0 and 1. It can be seen that with increasing the engine position the flutter speed is decreased. In this figure the stability flutter region is also shown.

Fig.15 demonstrates the 3D of the dimensionless flutter speed versus dimensionless engine position with triangle membership function for different α-cut. It can be interpreted that with increasing the uncertain input parameter bound, output behavior of flutter boundary getting away from the original triangle shape, especially when the engine position close to the tip of the wing.

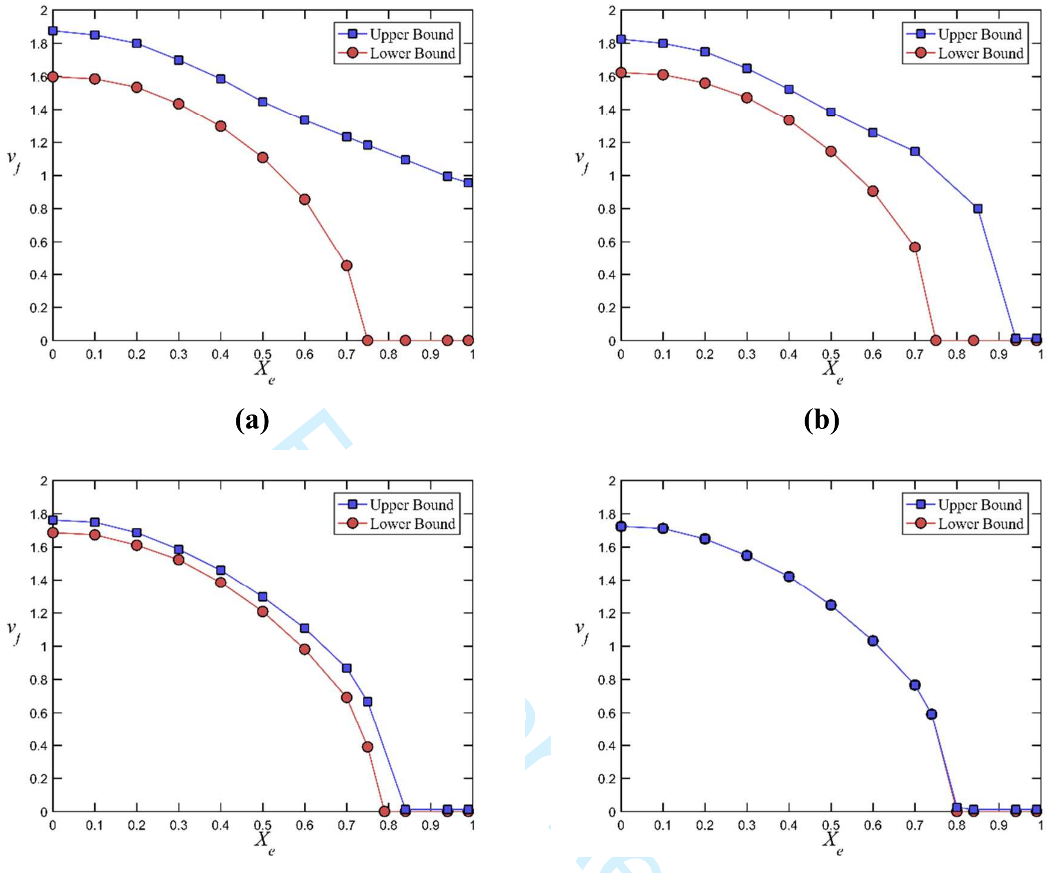

Figure 14. Dimensionless engine position vs dimensionless flutter speed with triangle membership functions for (a) α-cut=0; (b) α-cut=0.4; (c) α-cut=0.8, (d) α-cut=1.

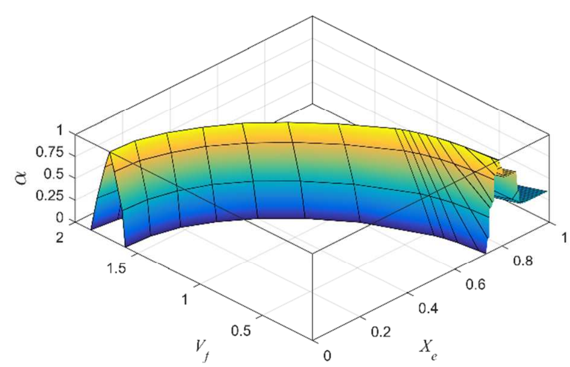

Figure 15. Dimensionless engine position vs dimensionless flutter speed in different α-cuts for triangle membership function.

7 CONCLUSION

Uncertainty analysis of the aircraft wing flutter predictions using fuzzy method is investigated. The wing model contains structural and aerodynamic uncertainties. These uncertain parameters are modelled as triangle and trapezium fuzzy membership functions and the α-cut method was employed to solve this fuzzy eigenvalue problem. Sensitivity and flutter analysis is carried out to identify the most influential parameters of the structure and aerodynamic models. Simulation results indicate that sensitivity to air density and lift curve slope is much larger than the sensitivity to geometric and structural parameters. In general, increasing the thrust force decreases the effects of lift curve slope and air density uncertainties on the flutter boundary. Furthermore, results show that although by increasing the thrust force, effects of the wing bending rigidity increases, but in general the impact of bending rigidity uncertainty on flutter boundary is low.

ACKNOWLEDGEMENT

Hamed Haddad Khodaparast acknowledges financial support from the Sêr Cymru National Research Network for Advanced Engineering and Materials (AEM - NRNC28) through industrial secondment award.

REFERENCES

[1] M. Goland, Y. L. Luke, The flutter of a uniform wing with tip weights, Journal of Applied Mechanics 15 (1) (1948) 13-20.

[2] I. Lottati, Aeroelastic stability characteristics of a composite swept wing with tip weights for an unrestrained vehicle, Journal of Aircraft 24 (1987) 793-802.

[3] F.H. Gern, L. Librescu, Effects of externally mounted stores on aeroelasticity of advanced aircraft wings, Journal of Aerospace Science and Technology 5 (1998) 321-333.

[4] D.H. Hodges, M.J. Patil, S. Chae, Effect of thrust on bending-torsion flutter of wings, Journal of Aircraft 39 (2) (2002) 371 – 376.

[5] S.A. Fazelzadeh, A. Mazidi and H. Kalantari, Bending-torsional flutter of wings with an attached mass subjected to a follower force, Journal of Sound and Vibration 323(1) (2009) 148 - 162.

[6] A. Mazidi, S.A. Fazelzadeh, P. Marzocca, Flutter of aircraft wings carrying a powered engine under roll maneuver, Journal of Aircraft 48 (3) (2011) 874 - 883.

[7] S.S. Rao, L. Berke, Analysis of uncertain structural systems using interval analysis, AIAA Journal. 35 (4) (1997) 727 - 735.

[8] R.L. Muhanna, R.L. Mullen, Uncertainty in mechanics problems interval based approach, Journal of Engineering Mechanics 127(6) (2001) 557 - 566.

[9] Z. Qiu, X. Wang, Comparison of dynamic response of structures with uncertain-but-bounded parameters using non-probabilistic interval analysis method and probabilistic approach, International Journal of Solids and Structures; 40(20) (2003) 5423 - 5439.

[10] Z. Qiu, Convex models and interval analysis method to predict the effect of uncertain-but-bounded parameters on the buckling of composite structures, Computer Methods in Applied Mechanics and Engineering; 194 (18) (2005) 2175 - 2189.

[11] R.L. Muhanna, H. Zhang and R.L. Mullen, Interval finite elements as a basis for generalized models of uncertainty in engineering mechanics, Reliable Computing 13(2) (2007) 173 - 194.

[12] H.Yun, J. Han, Robust flutter analysis of a nonlinear aeroelastic system with parametric uncertainties, Aerospace Science and Technology 13 (2-3) (2009) 139-149.

[13] S. Sarkar, J.A.S. Witteveen, A. Loeven, H. Bijl, Effect of uncertainty on the bifurcation behavior of pitching airfoil stall flutter, Journal of Fluids and Structures 25(2) (2009) 304-320.

[14] W. Xiaojun, Q. Zhiping, Interval finite element analysis of wing flutter, Chinese Journal of Aeronautics, 21(2) (2008) 134 - 140.

[15] H.H. Khodaparast, J.E. Mottershead, K.J. Badcock, Propagation of structural uncertainty to linear aeroelastic stability, Computers & Structures 88(3) (2010) 223-236.

[16] B.P. Danowsky, J.R. Chrstos, D.H. Klyde, C. Farhat, M. Brenner, Evaluation of aeroelastic uncertainty analysis methods. Journal of Aircraft 47 (4) (2010) 1266-1273.

[17] K.J. Badcock, S. Timme, S. Marques, H.H. Khodaparast, M.Prandina, J.E. Mottershead, A. Swift, A., A. Da Ronch, M.A. Woodgate, Transonic aeroelastic simulation for instability searches and uncertainty analysis, Progress in Aerospace Sciences 47(5) (2011) 392 - 423.

[18] Y. Yang, Z. Cai, Y. Liu. Interval analysis of dynamic response of structures using Laplace transform. Probabilistic Engineering Mechanics, 29, (2012)32-39.

[19] G. Muscolino, A. Sofi. Stochastic analysis of structures with uncertain-but-bounded parameters via improved interval analysis. Probabilistic Engineering Mechanics, 28, (2012) 152-163.

[20] Y. Gu, X. Zhang, Z. Yang, Robust flutter analysis based on genetic algorithm, Science China Technological Sciences (2012) 1-8.

[21] J.S. Song, J. Choo, S.J. Cha, S. Na, Z. Qin, Robust aeroelastic instability suppression of an advanced wing with model uncertainty in subsonic compressible flow field, Aerospace Science and Technology, 25 (1) (2013) 242-252.

[22] A.Sofi, G. Muscolino, I. Elishakoff, Natural frequencies of structures with interval parameters, Journal of Sound and Vibration, 347(2015) 79 - 95.

[23] C. Mannini, G. Bartoli, Aerodynamic uncertainty propagation in bridge flutter analysis, Structural Safety, 52 (2015) 29 - 39.

[24] T. Abbas, G. Morgenthal, Framework for sensitivity and uncertainty quantification in the flutter assessment of bridges, Probabilistic Engineering Mechanics 43 (2016) 91-105.

[25] S. Wu, E. Livne, Uncertainty analysis of flutter predictions with focus on the AGARD 445.6 wing, 58th AIAA/ASCE/AHS/ASC Structures, Structural Dynamics and Materials Conference, Grapevine, Texas (2017) 0412.

[26] M. Lokatt, Aeroelastic flutter analysis considering modeling uncertainties, Journal of Fluids and Structures, (2017), In Press.

[27] H. Zhao, Z. Gao, Y. Gao, C. Wang, Effective robust design of high lift NLF airfoil under multi-parameter uncertainty, Aerospace Science and Technology; 68 (2017) 530-542.

[28] J.T. Starczewski, Advanced Concepts in Fuzzy Logic and Systems with Membership Uncertainty, first ed., Springer, (2012).

[29] W.L. Chiang, W.M. Dong, F.S. Wong. Dynamic response of structures with uncertain parameters: A comparative study of probabilistic and fuzzy sets models. Probabilistic Engineering Mechanics, *2*(2) (1987) 82-91.

[30] F. Massa, B. Lallemand, T. Tison and P. Level, Fuzzy eigen solutions of mechanical structures, Engineering Computations; 21(1) (2004) 66 - 77.

[31] H. De Gersem, D. Moens, W. Desmet and D. Vandepitte, Interval and fuzzy dynamic analysis of finite element models with superelements, Computers & Structures 85(5) (2007) 304 - 319.

[32] I. Tartaruga; J.E. Cooper, G. Georgiou and H. Khodaparast, Flutter uncertainty quantification for the S4T model, AIAA Aerospace Sciences Meeting; 1; Texas; January, 1-13 (2017) 1653.

[33] H.H. Khodaparast, Y. Govers, I. Dayyani, S. Adhikari, M. Link, M.I. Friswell, J.E. Mottershead, J. Sienz, Fuzzy finite element model updating of the DLR AIRMOD test structure. Applied Mathematical Modelling (2017) https://doi.org/10.1016/j.apm.2017.08.001

[34] D.A. Peters, S. Karunamoorthy, W.M. Cao, Finite state induced flow models. I-Two-dimensional thin airfoil, Journal of Aircraft, 32 (2) (1995) 175 - 225.

[35] H.D. Hodges, G.A. Pierce, Introduction to Structural Dynamics and Aeroelasticity, second ed., Cambridge university press, New York, 2011.

[36] B.M. Ayyub, G.J. Klir, Uncertainty Modeling and Analysis in Engineering and the Sciences. ,first ed., CRC Press, 2006.

[37] F. Borello, E. Cestino, G. Frulla, Structural uncertainty effect on classical wing flutter characteristics. Journal of Aerospace Engineering, 23(4) (2010) 327-338.

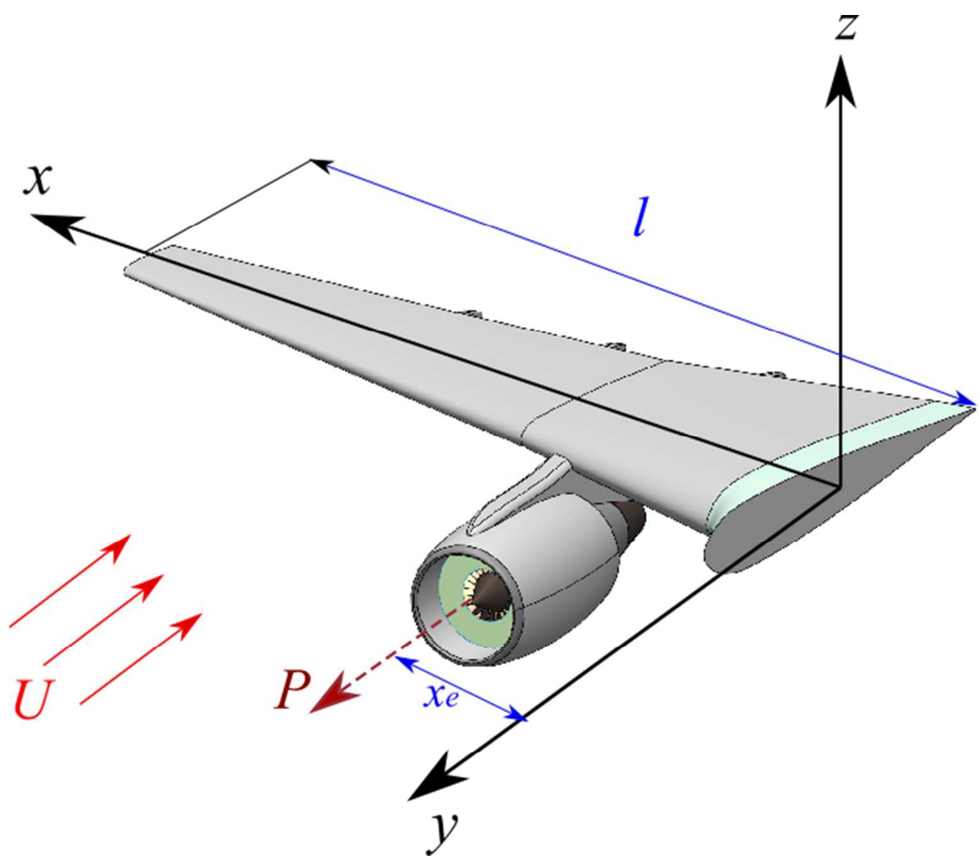

Figure 1. (a) Aircraft wing subjected to a thrust load, (b) the wing typical section.

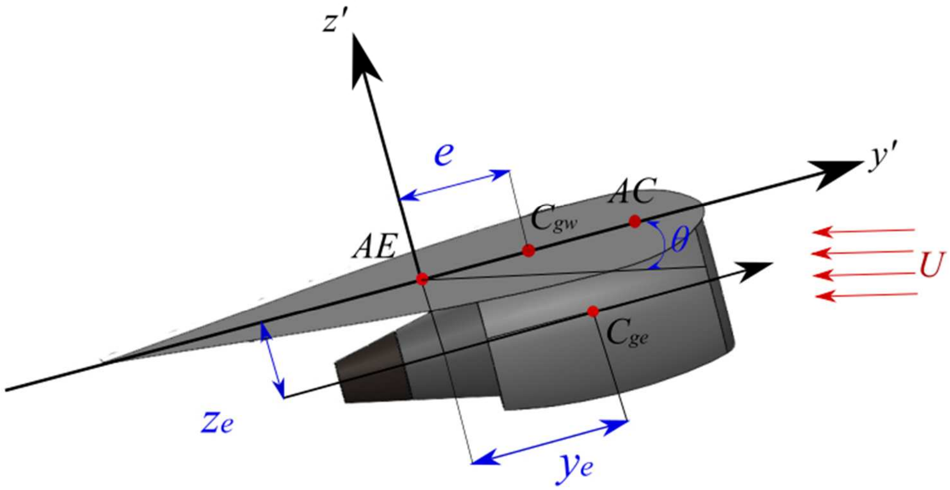

Figure 1. (a) Aircraft wing subjected to a thrust load,(b) the wing typical section.

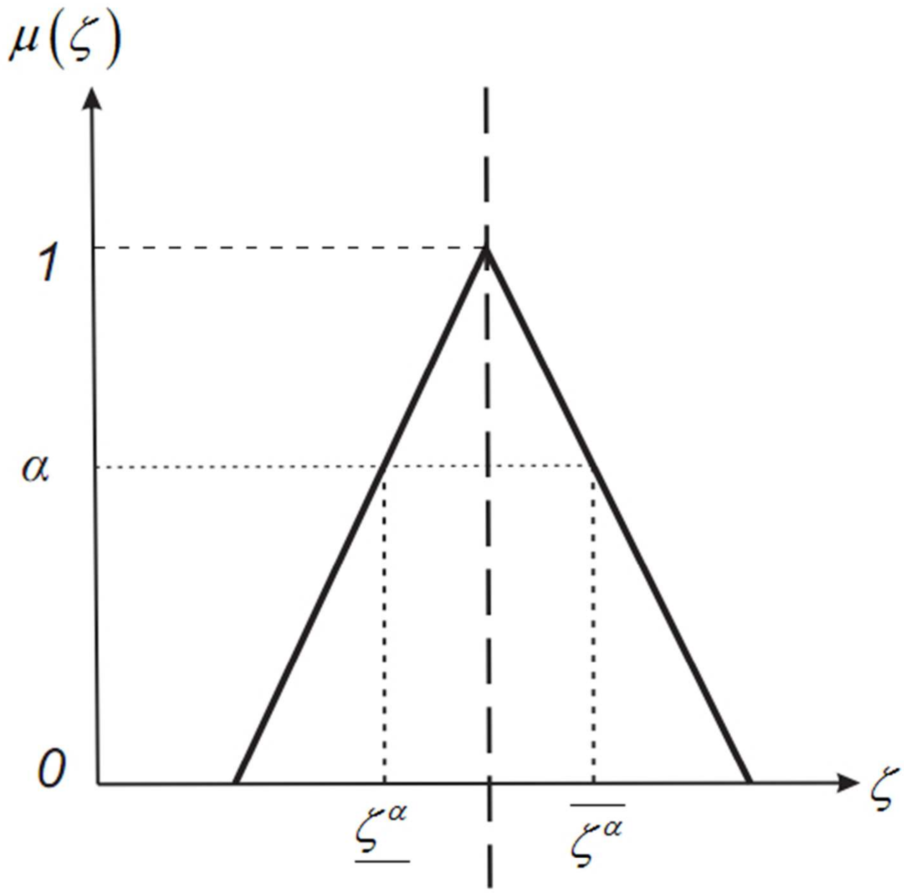

Figure 2. Fuzzy membership functions and (a) triangle (b) trapezium.

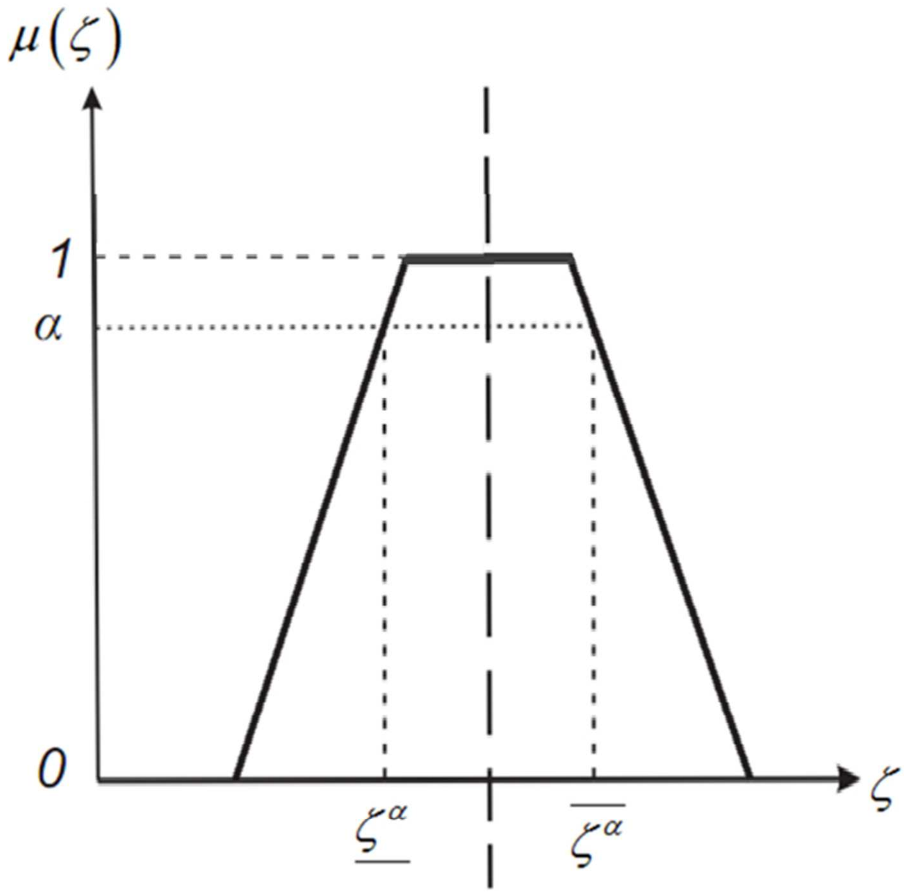

Figure 2. Fuzzy membership functions and (a) triangle (b) trapezium.

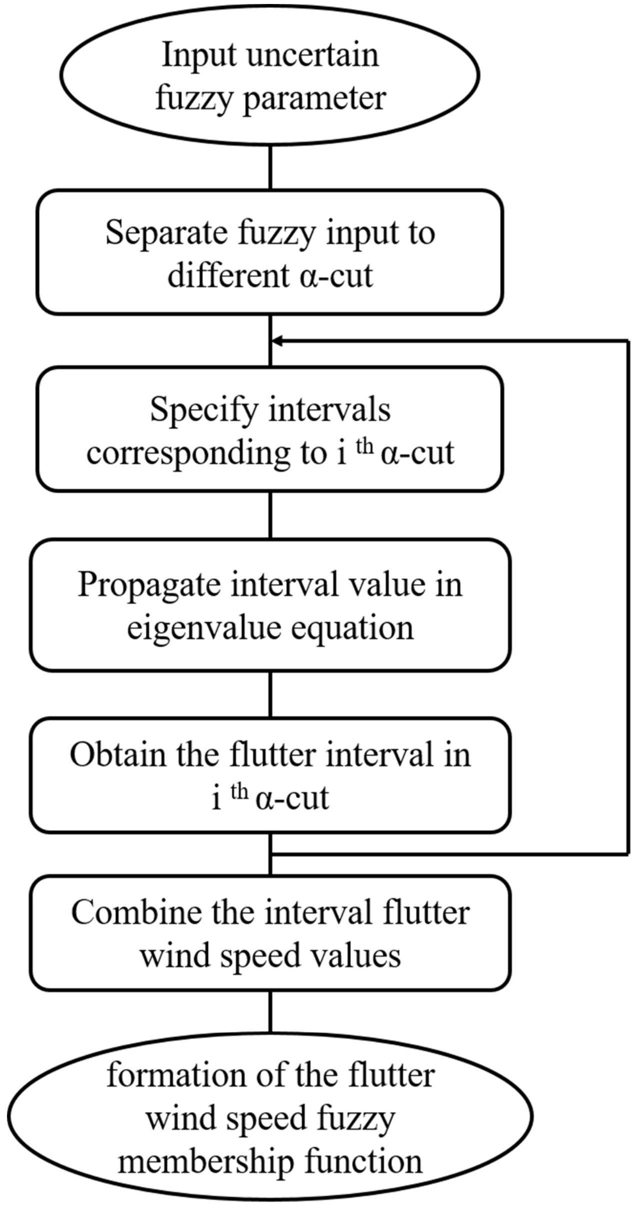

Figure 3. The flowchart of fuzzy interval method.

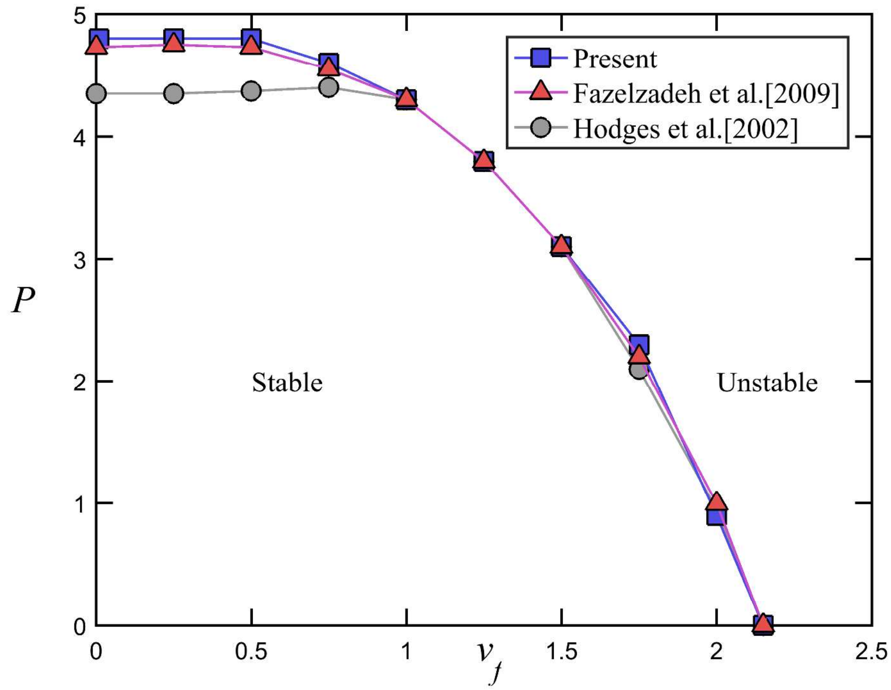

Figure 4. Flutter boundary of a clean wing subjected to thrust force.

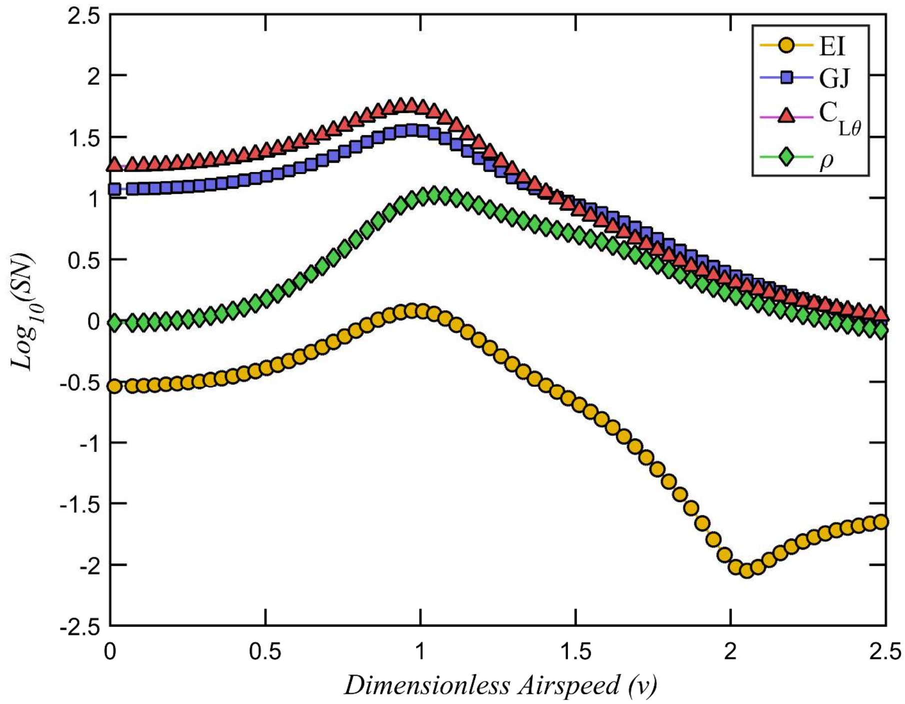

Figure 5. Dimensionless sensitivity vs dimensionless airspeed at P=4.5.

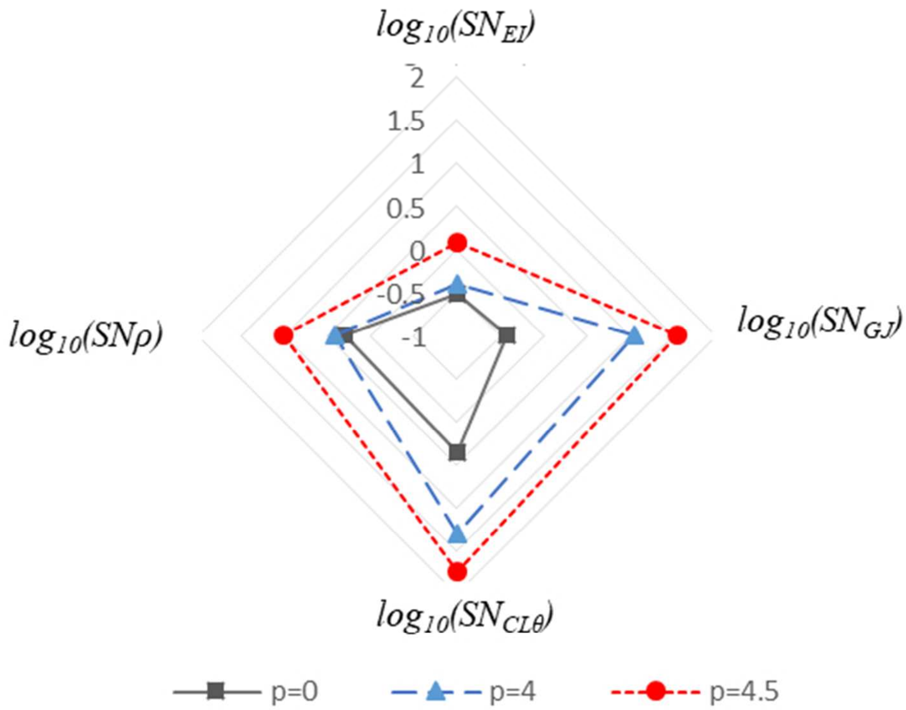

Figure 6. Dimensionless sensitivity at flutter speed for different dimensionless thrust forces.

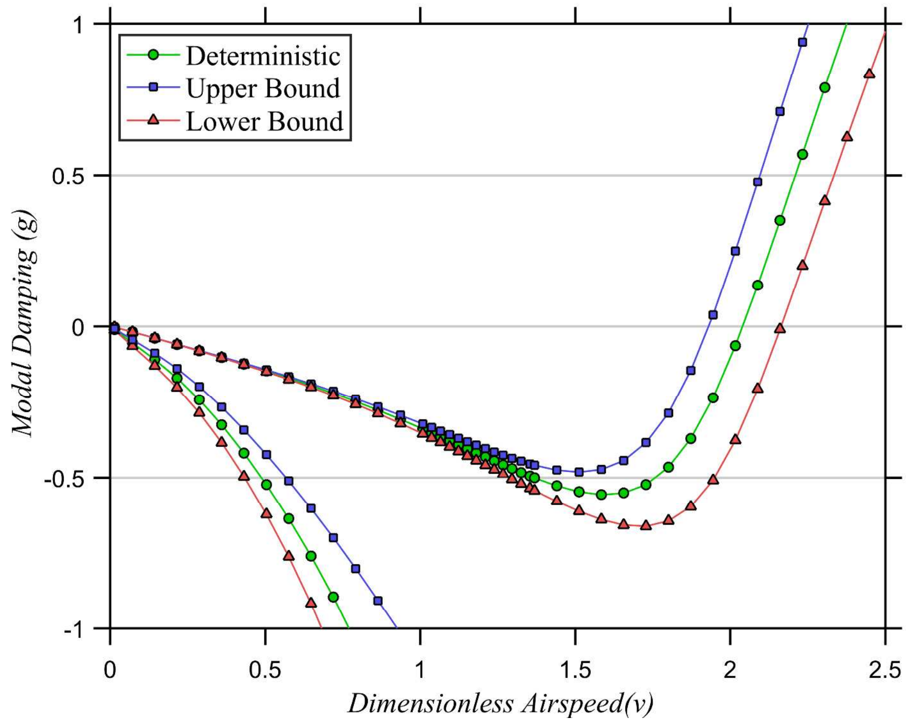

Figure 7. Modal damping vs dimensionless airspeed for different thrust forces (a) α-cut=0, P=0; (b) α-cut=0, P=4; (c)α-cut=0.5, P=0; (d)α-cut=0.5, P=4.

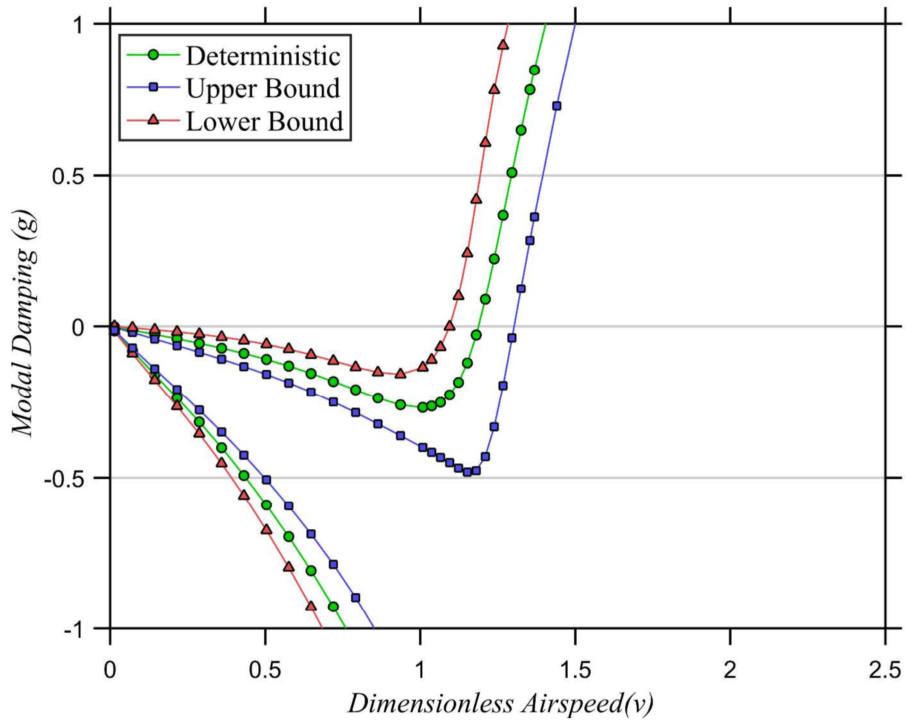

Figure 7. Modal damping vs dimensionless airspeed for different thrust forces (a) α-cut=0, P=0; (b) α-cut=0, P=4; (c)α-cut=0.5, P=0; (d)α-cut=0.5, P=4.

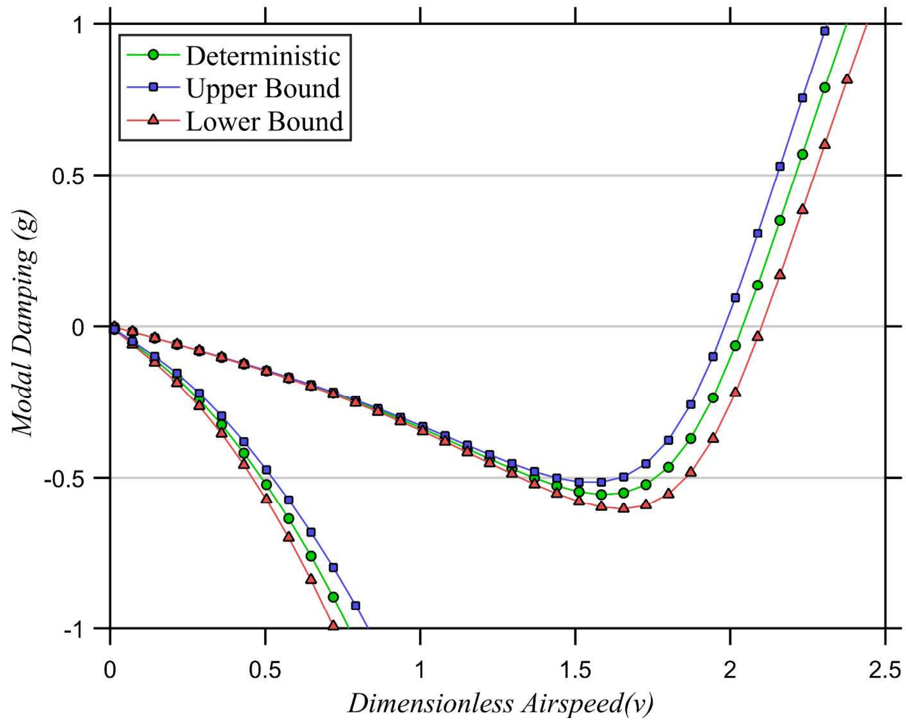

Figure 7. Modal damping vs dimensionless airspeed for different thrust forces (a) α-cut=0, P=0; (b) α-cut=0, P=4; (c)α-cut=0.5, P=0; (d)α-cut=0.5, P=4.

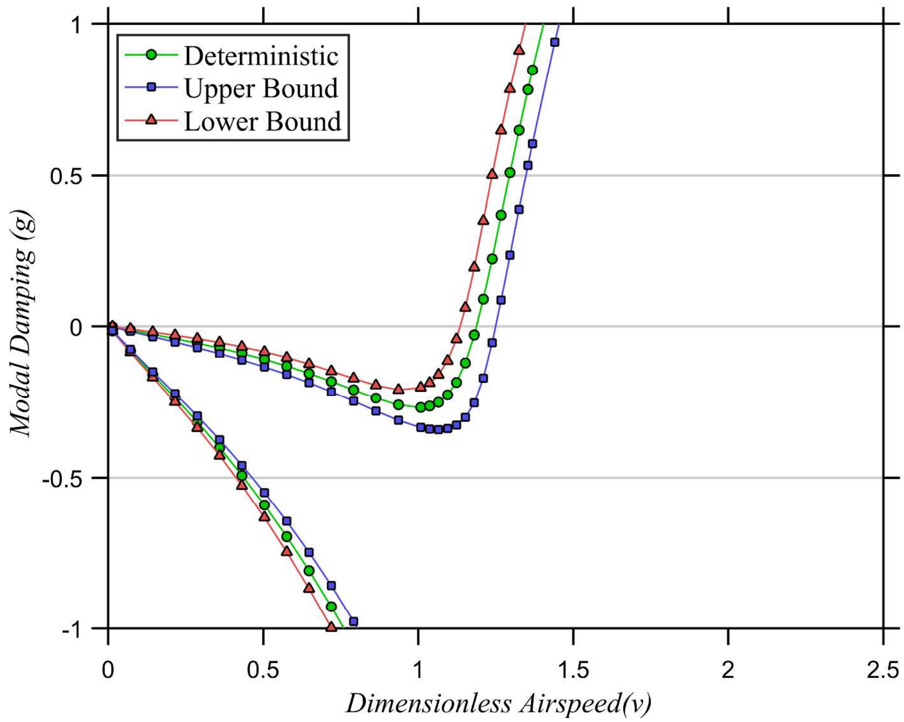

Figure 7. Modal damping vs dimensionless airspeed for different thrust forces (a) α-cut=0, P=0; (b) α-cut=0, P=4; (c)α-cut=0.5, P=0; (d)α-cut=0.5, P=4.

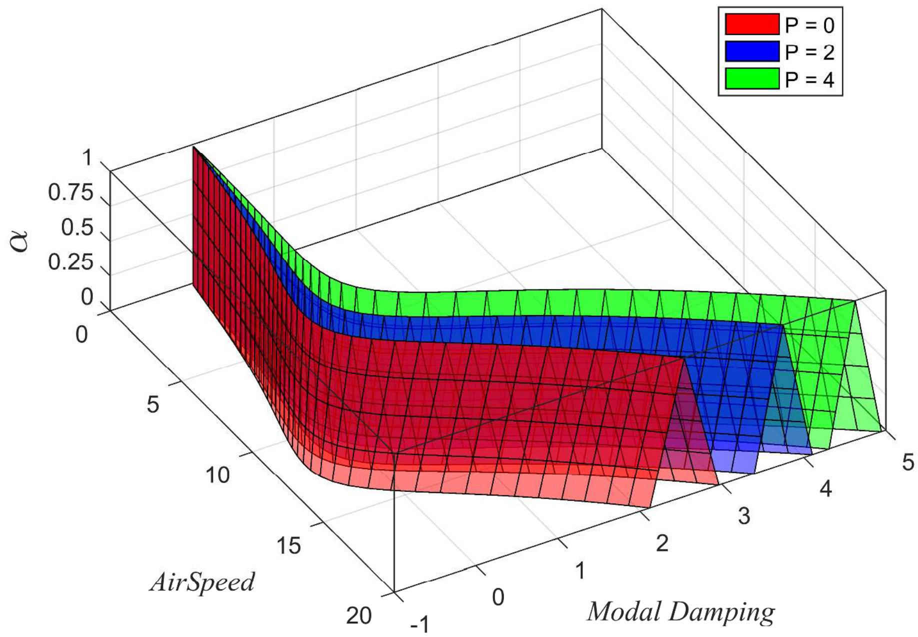

Figure 8.Modal damping vs airspeed in different α-cuts at P=0, 2, 4.

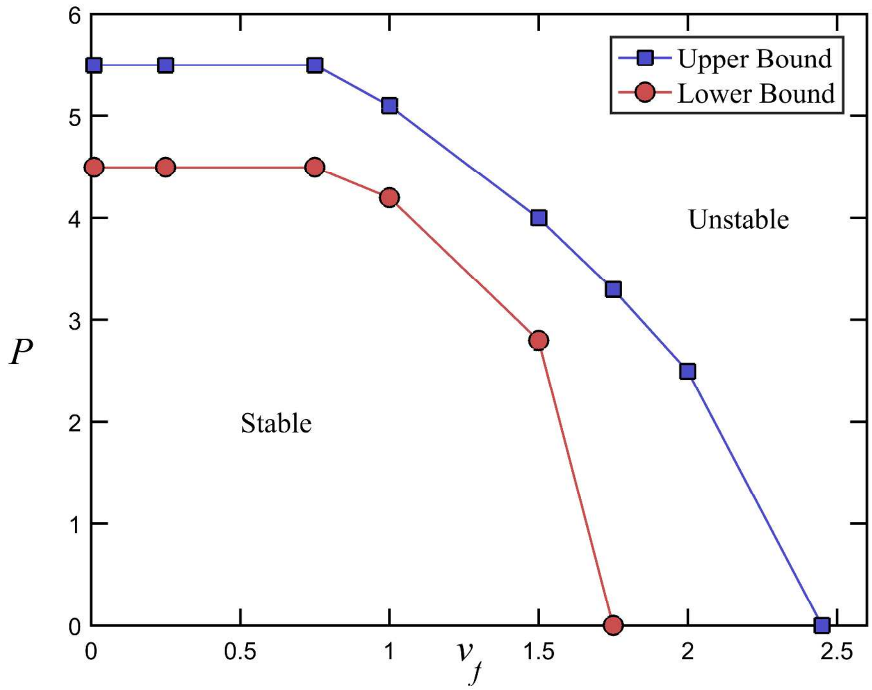

Figure 9. Thrust force vs flutter speed with triangle membership functions for (a) α-cut=0; (b) α-cut=0.4; (c) α-cut=0.8, (d)α-cut=1.

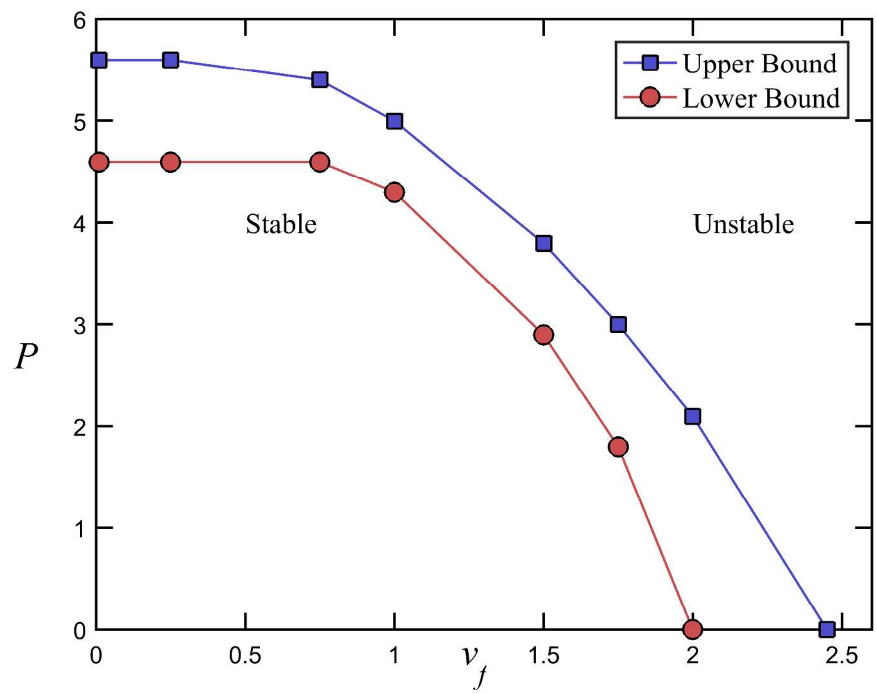

Figure 9. Thrust force vs flutter speed with triangle membership functions for (a) α-cut=0; (b) α-cut=0.4; (c) α-cut=0.8, (d)α-cut=1.

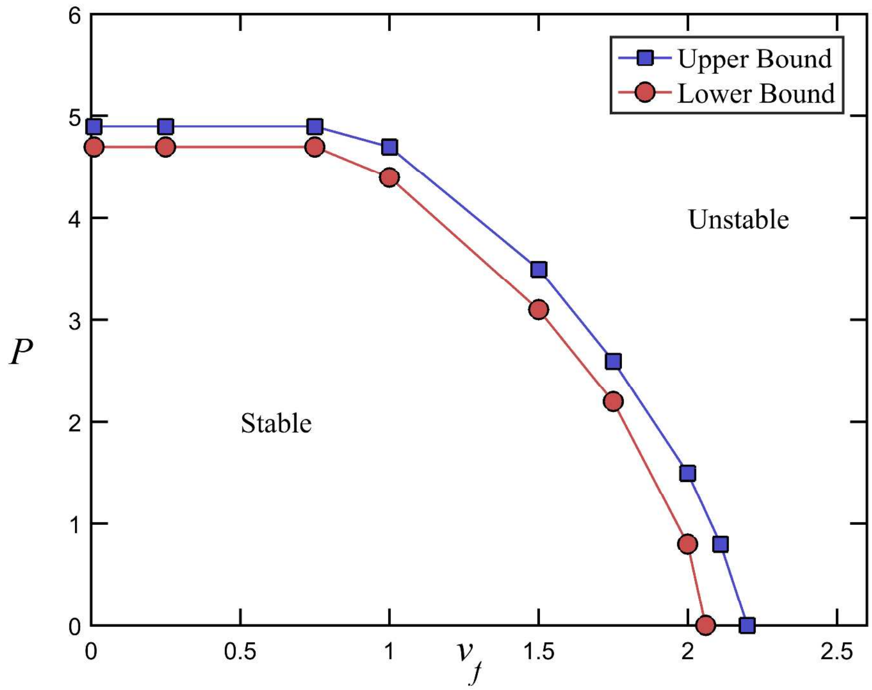

Figure 9. Thrust force vs flutter speed with triangle membership functions for (a) α-cut=0; (b) α-cut=0.4; (c) α-cut=0.8, (d)α-cut=1.

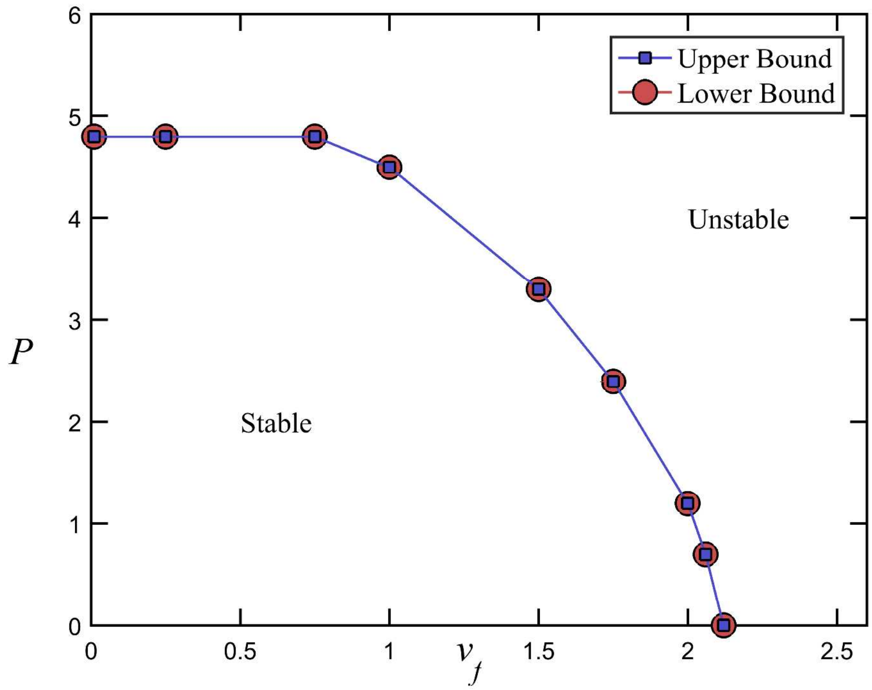

Figure 9. Thrust force vs flutter speed with triangle membership functions for (a) α-cut=0; (b) α-cut=0.4; (c) α-cut=0.8, (d)α-cut=1.

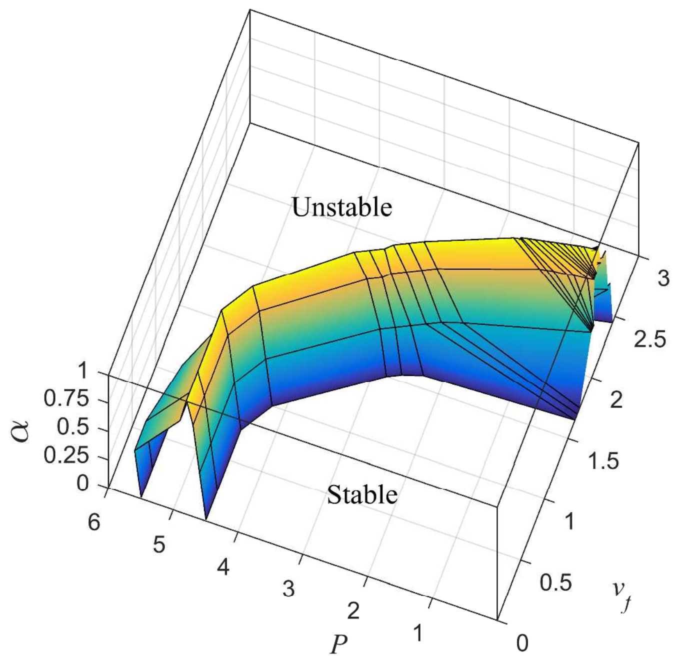

Figure 10. Thrust force vs flutter speed in different α-cuts for triangle membership function.

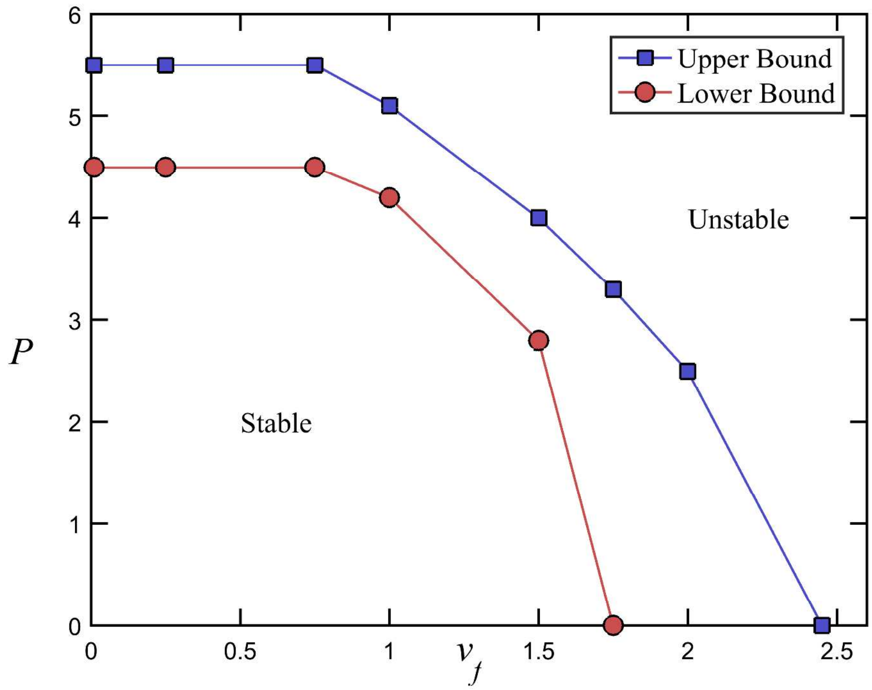

Figure 11. Thrust force vs flutter speed trapezium membership function (a) α-cut=0; (b) α-cut=0.4; (c) α-cut=0.6, (d) α-cut=1.

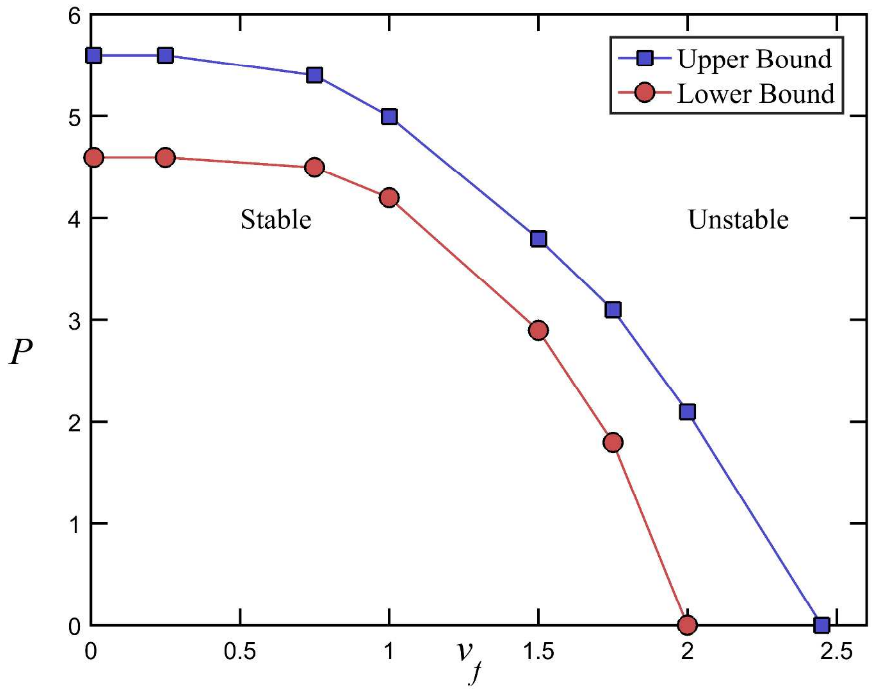

Figure 11. Thrust force vs flutter speed trapezium membership function (a) α-cut=0; (b) α-cut=0.4; (c) α-cut=0.6, (d) α-cut=1.

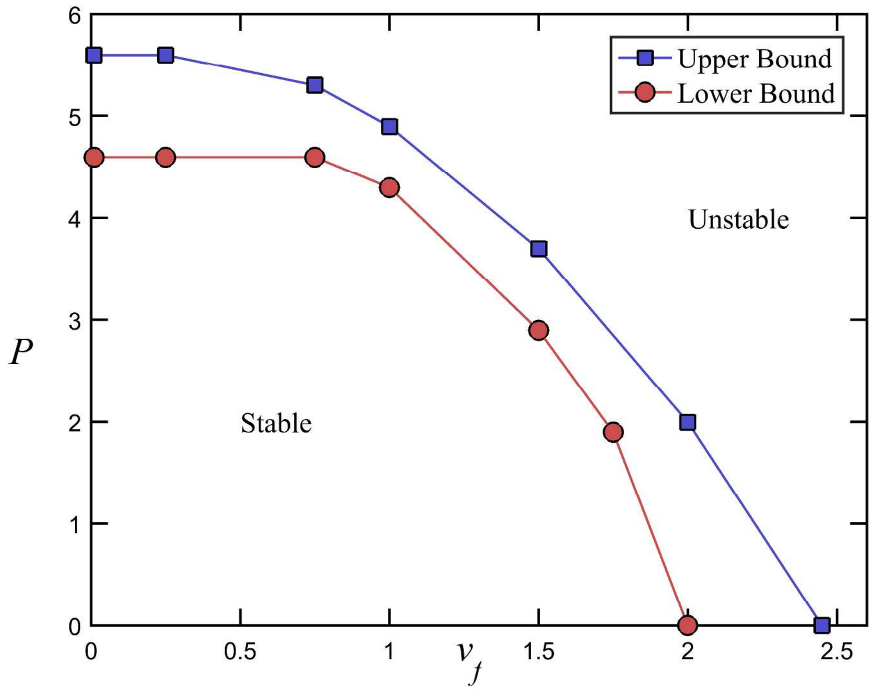

Figure 11. Thrust force vs flutter speed trapezium membership function (a) α-cut=0; (b) α-cut=0.4; (c) α-cut=0.6, (d) α-cut=1.

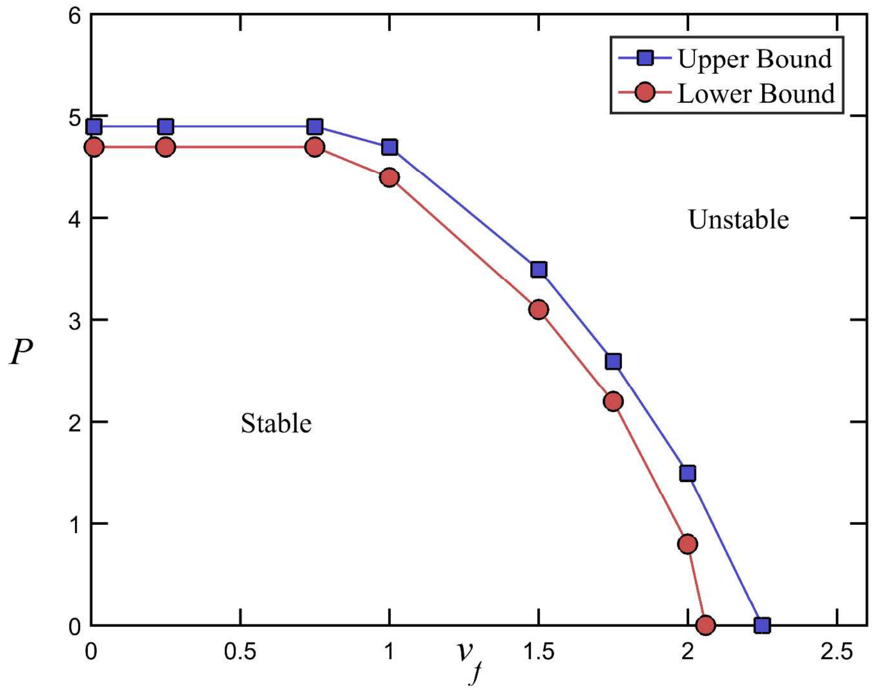

Figure 11. Thrust force vs flutter speed trapezium membership function (a) α-cut=0; (b) α-cut=0.4; (c) α-cut=0.6, (d) α-cut=1.

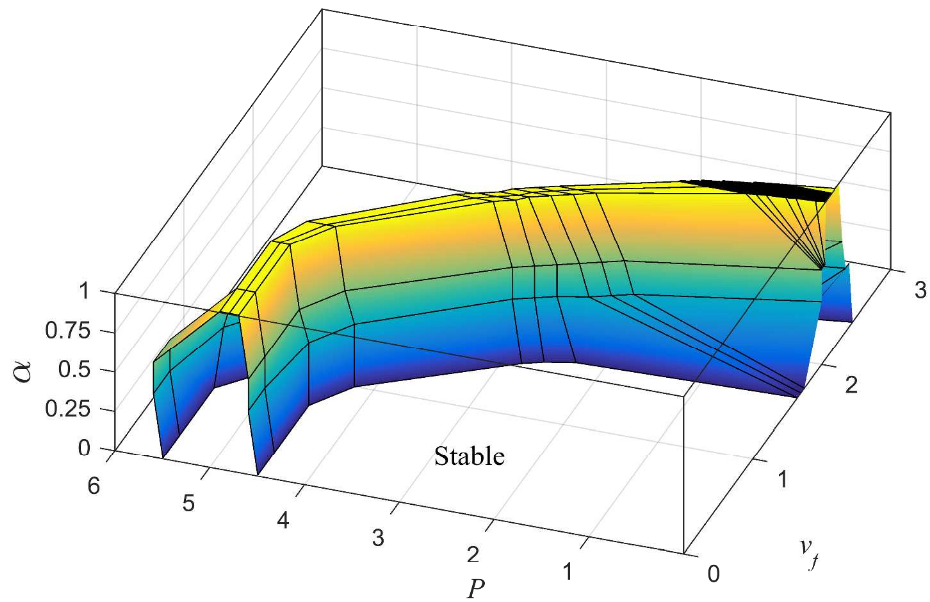

Figure 12. Thrust force vs flutter speed in different α-cuts for trapezium membership functions.

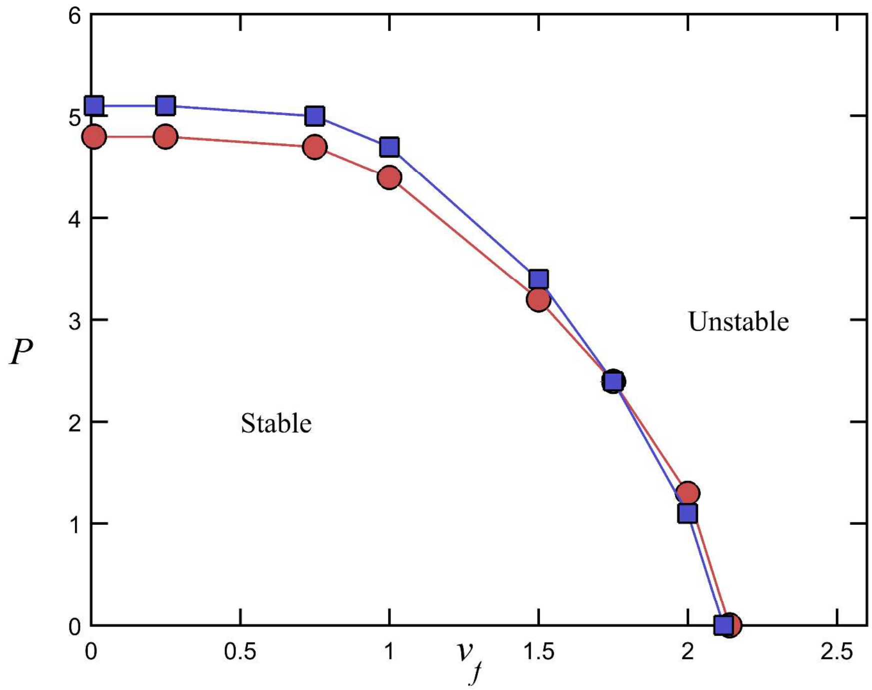

Figure 13. Thrust force vs Flutter speed in α-cut= 0 for uncertain parameter (a) EI ; (b) GJ; (c)CLθ ; (d) ρ.

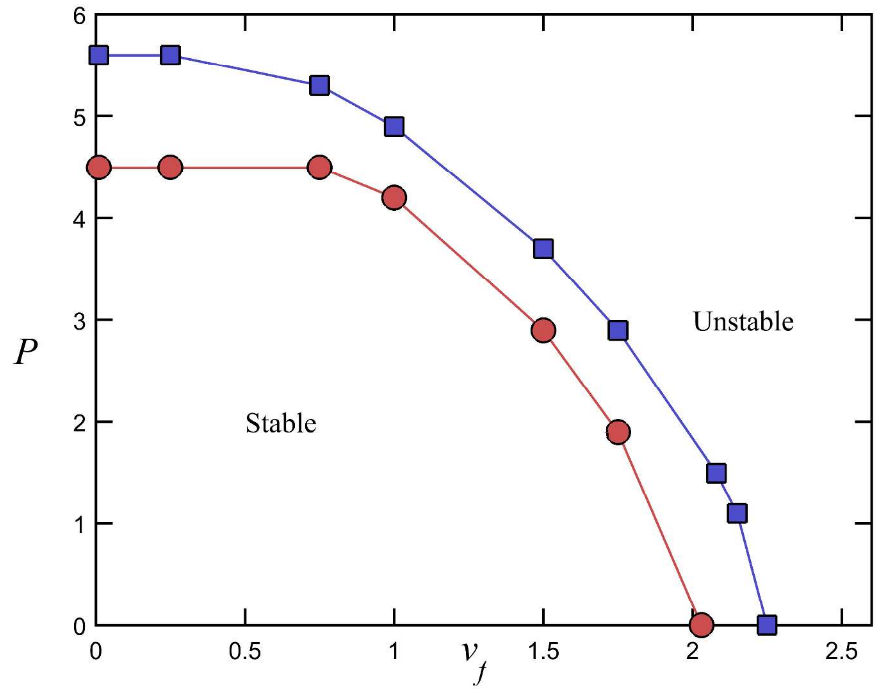

Figure 13. Thrust force vs Flutter speed in α-cut= 0 for uncertain parameter (a) EI ; (b) GJ; (c)CLθ ; (d) ρ.

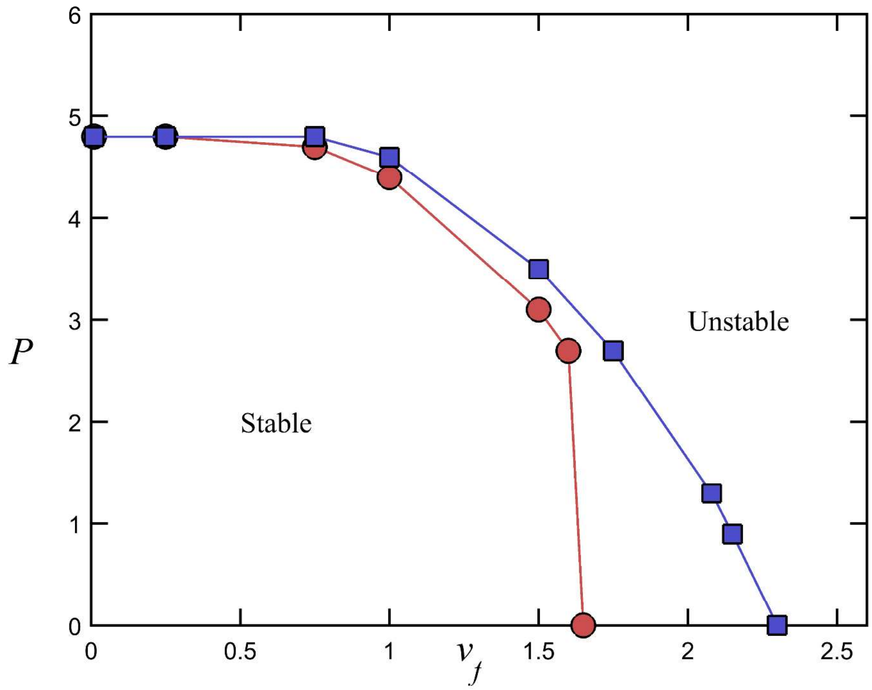

Figure 13. Thrust force vs Flutter speed in α-cut= 0 for uncertain parameter (a) EI ; (b) GJ; (c)CLθ ; (d) ρ.

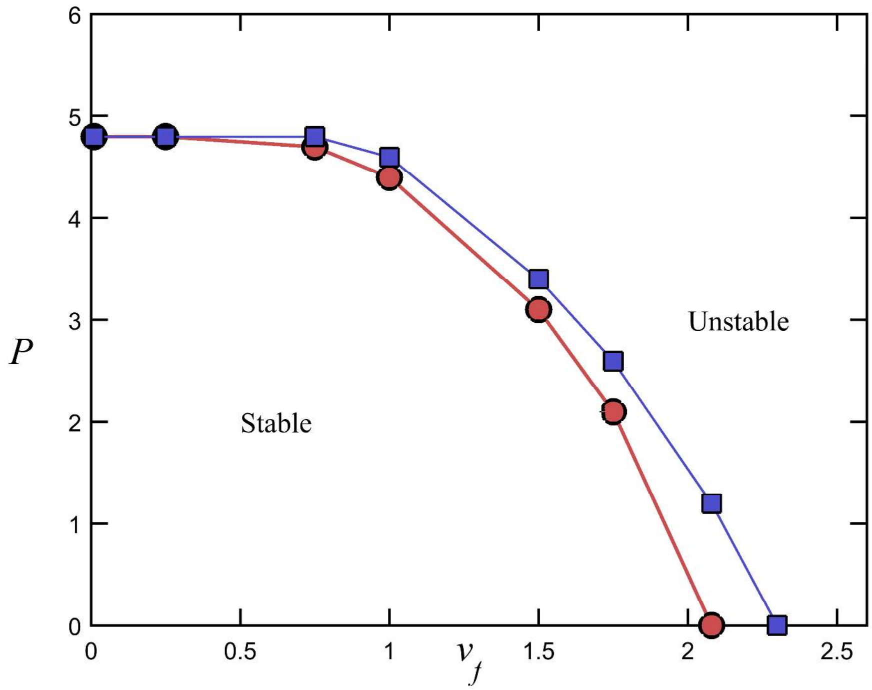

Figure 13. Thrust force vs Flutter speed in α-cut= 0 for uncertain parameter (a) EI ; (b) GJ; (c)CLθ ; (d) ρ.

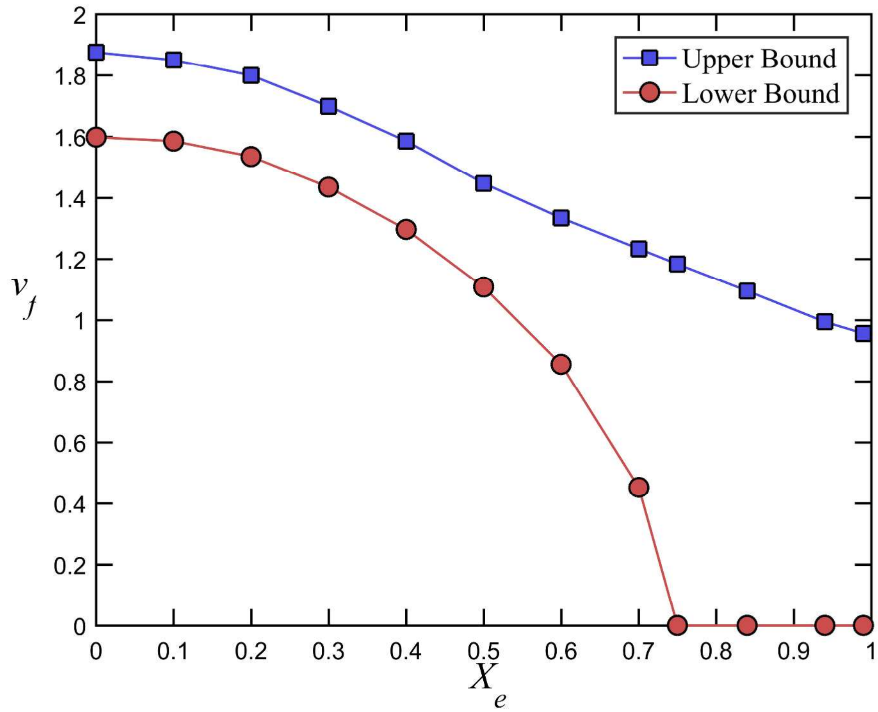

Figure 14. Dimensionless engine position vs dimensionless flutter speed with triangle membership functions for (a) α-cut=0; (b) α-cut=0.4; (c) α-cut=0.8, (d) α-cut=1.

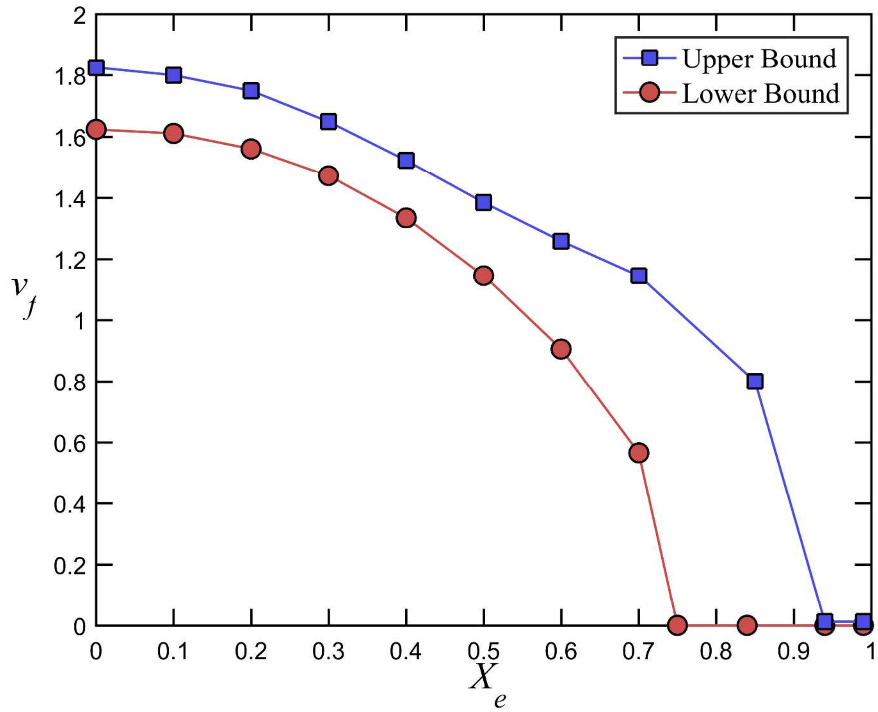

Figure 14. Dimensionless engine position vs dimensionless flutter speed with triangle membership functions for (a) α-cut=0; (b) α-cut=0.4; (c) α-cut=0.8, (d) α-cut=1.

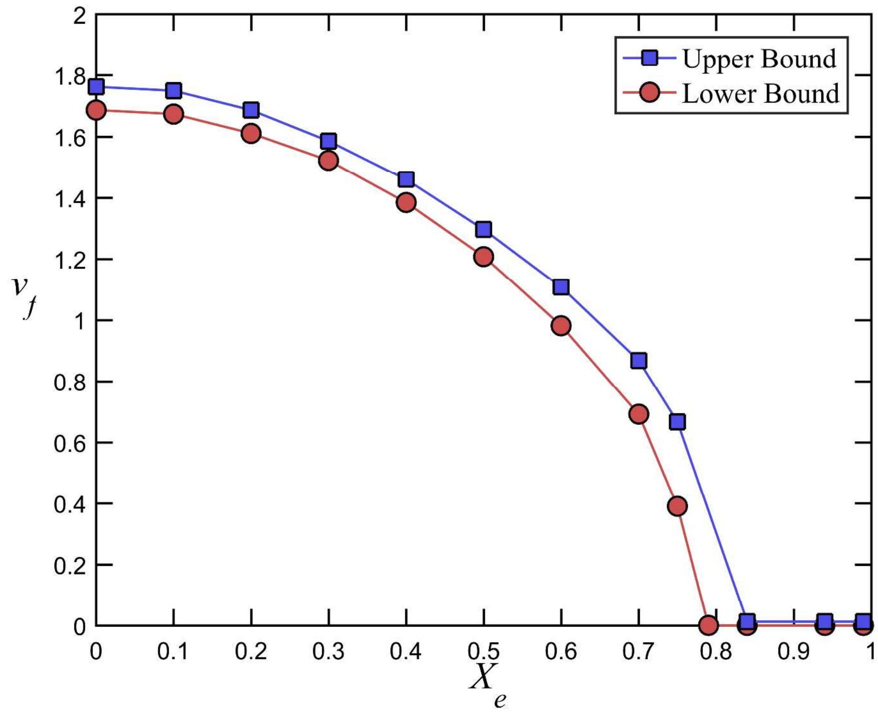

Figure 14. Dimensionless engine position vs dimensionless flutter speed with triangle membership functions for (a) α-cut=0; (b) α-cut=0.4; (c) α-cut=0.8, (d) α-cut=1.

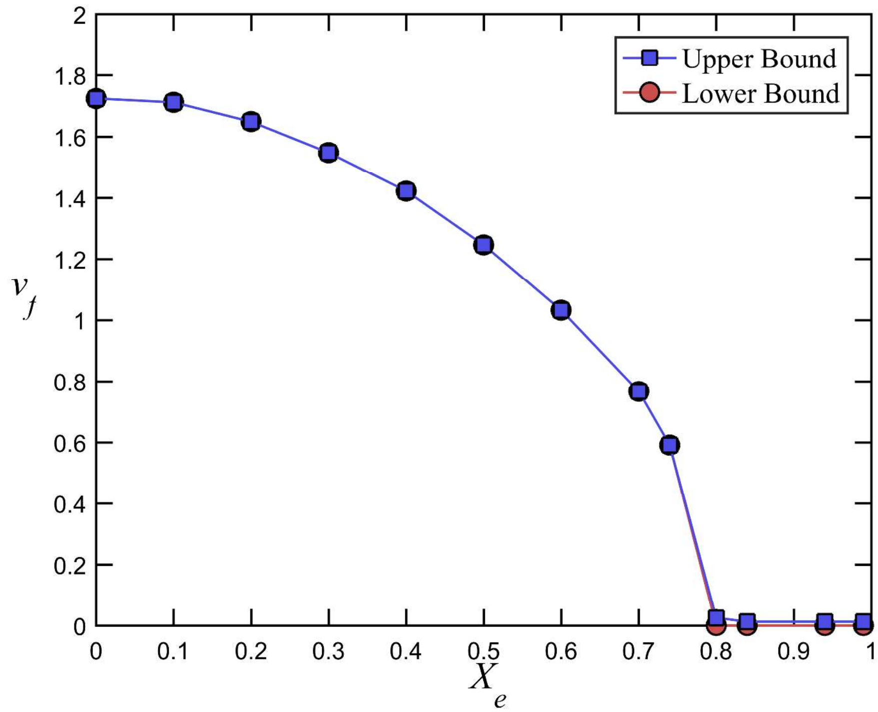

Figure 14. Dimensionless engine position vs dimensionless flutter speed with triangle membership functions for (a) α-cut=0; (b) α-cut=0.4; (c) α-cut=0.8, (d) α-cut=1.

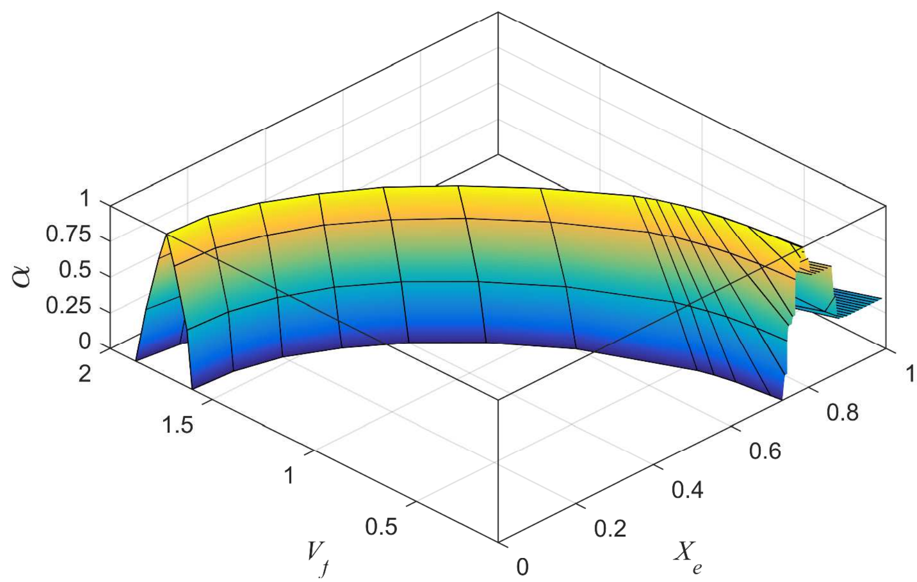

Figure 15. Dimensionless engine position vs dimensionless flutter speed in different α-cuts for triangle membership function.

Figure 1. (a) Aircraft wing subjected to a thrust load, (b) the wing typical section.

Figure 2. Fuzzy membership functions and (a) triangle (b) trapezium.

Figure 3. The Flowchart of Fuzzy interval Method.

Figure 4. Flutter boundary of a clean wing subjected to thrust force.

Figure 5. Dimensionless sensitivity vs dimensionless airspeed at P=4.5.

Figure 6. Dimensionless sensitivity at flutter speed for different dimensionless thrust forces.

Figure 7. Modal damping vs dimensionless airspeed for different thrust forces (a) α-cut=0, P=0; (b) α-cut=0, P=4; (c)α-cut=0.5, P=0; (d)α-cut=0.5, P=4.

Figure 8.Modal damping vs airspeed in different α-cuts at P=0, 2, 4.

Figure 9. Thrust force vs flutter speed with triangle membership functions for (a) α-cut=0; (b) α-cut=0.4; (c) α-cut=0.8, (d)α-cut=1.

Figure 10. Thrust force vs flutter speed in different α-cuts for triangle membership functions.

Figure 11. Thrust force vs flutter speed trapezium membership function (a) α-cut=0; (b) α-cut=0.4; (c) α-cut=0.6, (d) α-cut=1.

Figure 12. Thrust force vs flutter speed in different α-cuts for trapezium membership functions.

Figure 13. Thrust force vs Flutter speed in α-cut= 0 for uncertain parameter (a) EI ; (b) GJ; (c) ; (d) ρ.

Figure 14. Dimensionless engine position vs dimensionless flutter speed with triangle membership functions for (a) α-cut=0; (b) α-cut=0.4; (c) α-cut=0.8, (d) α-cut=1.

Figure 15. Dimensionless engine position vs dimensionless flutter speed in different α-cuts for triangle membership function.

Table 1: The wing model characteristics [4].

Parameters	Value
Wing Length	16 m
Semi-chord	0.5 m
Bending rigidity	2e4 N.m^2
Torsional rigidity	2e3 N.m^2
Mass per unit length	0.75 Kg/m
Wing moment of inertia	0.1 Kg.m

Table 1: Deterministic flutter speed and frequency comparison

Refrence	Flutter Speed(m/s)	Error (%)	Frequency Flutter(Hz)	Error(%)
Goland and Luke[1]	494.1	-	11.25	-
Gern and Liberscu[3]	493.6	-0.1	12.02	6.84
Fazelzadeh et al [5].	493.4	-0.14	12.02	6.84
Borello et al.[37]	508.2	2.85	11.55	2.67
Present	494.3	0.04	11.33	0.07

Table 1: Uncertain fuzzy parameters (Triangle membership function).

Parameters	Minimum Value	Crisp Value	Maximum Value	Percentage of Variation
Bending Rigidity	19000	20000	21000	±5%
Torsional Rigidity	1900	2000	2100	±5%
Air Density	0.0845	0.0889	0.0933	±5%
Lift Curve Slope	5.3058	5.5851	5.8643	±5%

Table 1: Uncertain fuzzy parameters (Trapezium membership function).

Parameters	Minimum Value	Minimum Middle value	Crisp Value	Maximum Middle value	Maximum Value	Percentage of Variation
Bending Rigidity	19000	19800	20000	20200	21000	±5%
Torsional Rigidity	1900	1980	2000	2020	2100	±5%
Air Density	0.0845	0.088	0.0889	0.0898	0.0933	±5%
Lift Curve Slope	5.3058	5.5292	5.5851	5.6409	5.8643	±5%